5. Electrical Transport

CONTENTS

5.1 Quasi-Classical Approach 203
5.2 Carrier Mobility for a Nondegenerate Electron Gas 206
5.3 Modulation Doping 223
5.4 High-Field Transport and Hot Carrier Effects 225
5.5 Magneto-Transport and the Hall Effect 232
Problems 237
Summary 241

In Chap. 4 we studied electrons and holes located around defects. Since these electrons and holes are immobile they are known as **bound** *electrons and holes*, respectively. In contrast, electrons in the conduction band and holes in the valence band of a semiconductor can carry electrical current. Hence they are referred to as **free carriers**. In this chapter we will study the effect of an external electric field on free carriers in a semiconductor. The response of these carriers to an electric field depends on the field strength. We will first consider the case of weak electric fields, where the behavior of carriers can be described by **Ohm's law**. Under high electric fields, carriers in a semiconductor can acquire so much energy that their average kinetic energy becomes higher than that of the lattice. Such energetic electrons are known as **hot electrons**. It is very difficult to calculate their properties analytically, therefore our discussions of hot electrons will be qualitative.

5.1 Quasi-Classical Approach

Let $\boldsymbol{F}$ represent a weak external static electric field applied to a semiconductor. We can assume without loss of generality, that this semiconductor contains only free electrons (i. e., it is an n-*type* semiconductor). For simplicity, we will assume that the concentration of free electrons is low enough that we can neglect their interactions with each other (such as collision and screening effects). We will also neglect local field effects due to ionic charges, i. e. the field experienced by every free electron is assumed to be equal to the external applied field. Now let Φ be the electric potential associated with the applied

field. The wave equation for the time evolution of an electron in a semiconductor under the influence of Φ is given by

$$(H_0 - e\Phi)\psi(\boldsymbol{r}, t) = \mathrm{i}\hbar \frac{\partial \psi}{\partial t}, \tag{5.1}$$

where H_0 is the one-electron Hamiltonian (in the absence of external perturbations) that we have already studied in Sect. 2.1, e is the magnitude of the electronic charge and $\psi(\boldsymbol{r}, t)$ is the electron wave function in the presence of the external field. As long as Φ is small and does not vary rapidly in space, we can use the effective mass approximation (Sect. 4.2.1) to solve (5.1). The approach is very similar to the way we handled the donor electron problem in Sect. 4.2. The difference is that, in the present case, we are interested in the nonstationary solutions, which produce a current in response to the applied field. This requires the expectation value of $e\boldsymbol{v}$ to be evaluated where $\boldsymbol{v}$ is the electron velocity operator. The current density operator $\boldsymbol{j}$ is then defined as

$$\boldsymbol{j} = ne\boldsymbol{v}, \tag{5.2}$$

where n is the electron density. As we saw in Sect. 4.2, solving the Schrödinger equation within the effective mass approximation is quite an involved process. Instead of the fully quantum mechanical approach, we will adopt here a quasi-classical approach [5.1]. We shall derive a classical equation of motion for our electron in the external field based on the effective mass approximation.

As we discussed in detail in Sect. 4.2.1, a wave equation for Bloch waves such as (5.1) can be replaced by an effective wave equation for the envelope functions $C(\boldsymbol{R}, t)$. For simplicity we shall assume that our electron is in an isotropic and nondegenerate conduction band with an energy minimum at the zone center ($\boldsymbol{k} = 0$) and a dispersion given by

$$E_{\mathrm{c}}(\boldsymbol{k}) = E_{\mathrm{c}}(0) + \frac{\hbar^2 k^2}{2m^*}, \tag{5.3}$$

where m^* is the effective mass. These assumptions are valid for electrons in direct bandgap semiconductors such as GaAs and InP but not for Si and Ge. Within the effective mass approximation the wave equation for the envelope functions can be written as [see (4.22)]

$$\left[E_{\mathrm{c}}(0) - \left(\frac{\hbar}{2m^*}\right)\frac{\partial^2}{\partial \boldsymbol{R}^2} - e\Phi(\boldsymbol{R})\right] C(\boldsymbol{R}, t) \approx \mathrm{i}\frac{\hbar\partial}{\partial t} C(\boldsymbol{R}, t). \tag{5.4}$$

Instead of solving (5.4), we argue that the net effect of the crystal potential on the motion of this electron inside the semiconductor is to cause its mass to change from the value in free space to m^*. This suggests that, as a simple approximation, we can describe the motion of this electron in an external electric field by a classical equation of motion (see, for example, [5.1])

$$m^* \frac{d^2\boldsymbol{r}}{dt^2} + \frac{m^*}{\tau}\left(\frac{d\boldsymbol{r}}{dt}\right) = -e\boldsymbol{F}, \tag{5.5}$$

where $\boldsymbol{r}$ is the position of the electron and τ is a phenomenological scattering time introduced to account for the scattering of the electron by impurities and phonons. Equation (5.5) is considered quasi-classical because the concept of an effective mass for the electron motion has been derived quantum mechanically.

Once we have established (5.5), the motion of any charge q can be derived via classical mechanics. For example, under the influence of $\boldsymbol{F}$ a stationary charge will accelerate. As its velocity increases, the retardation term $(m^*/\tau)(d\boldsymbol{r}/dt)$ will also increase. Eventually the retardation term will cancel the term due to $\boldsymbol{F}$ and a steady state in which the charge has no acceleration is attained. The steady-state velocity of the charge is known as its **drift velocity** $\boldsymbol{v}_\mathrm{d}$. It is obtained from (5.5) by setting the acceleration term $m^*(d^2\boldsymbol{r}/dt^2)$ to zero and denoting by q the electronic charge $-e$:

$$\boldsymbol{v}_\mathrm{d} = q\boldsymbol{F}\tau/m^*. \tag{5.6}$$

The current density $\boldsymbol{J}$ at steady state is related to $\boldsymbol{v}_\mathrm{d}$ by

$$\boldsymbol{J} = nq\boldsymbol{v}_\mathrm{d}. \tag{5.7}$$

Combining (5.6 and 7) we obtain an expression for the current density:

$$\boldsymbol{J} = nq^2\boldsymbol{F}\tau/m^*. \tag{5.8}$$

The second-rank **conductivity tensor** $\boldsymbol{\sigma}$ is defined in general by

$$\boldsymbol{J} = \boldsymbol{\sigma} \cdot \boldsymbol{F}. \tag{5.9}$$

For the case of an isotropic conduction band $\boldsymbol{\sigma}$ is a diagonal tensor with all diagonal elements given by

$$\sigma = nq^2\tau/m^*. \tag{5.10}$$

Since σ depends on q^2, the contributions to the conductivity of a semiconductor from electrons and holes always add. Semiconductors differ from metals in that their carrier densities can be varied widely by changing the temperature or the dopant concentration. It is therefore convenient to factor out the dependence of σ on n. This can be accomplished by defining a carrier **mobility** μ as

$$\boldsymbol{v}_\mathrm{d} = \mu\boldsymbol{F}. \tag{5.11}$$

Combining (5.6 and 11) we obtain

$$\mu = q\tau/m^*. \tag{5.12}$$

In a semiconductor containing both free electrons and free holes σ is given by

$$\sigma = e(n_\mathrm{e}\mu_\mathrm{e} + n_\mathrm{h}\mu_\mathrm{h}), \tag{5.13}$$

where the subscripts e and h refer to electrons and holes, respectively.

5.2 Carrier Mobility for a Nondegenerate Electron Gas

The expressions we derived in the previous section are valid when all the carriers have the same scattering time. We will now generalize these expressions to the case where the carriers are distributed in a band according to the Boltzmann distribution [to be defined later in (5.22)] and the scattering time depends on the carrier energy.

5.2.1 Relaxation Time Approximation

We define the **distribution function** $f_{\boldsymbol{k}}(\boldsymbol{r})$ of a carrier as the probability that a band state with energy $E_{\boldsymbol{k}}$ will be occupied by this carrier at a carrier temperature T. We assume that in the absence of an external field the carriers are at thermal equilibrium, so that $f_{\boldsymbol{k}}$ is equal to the **Fermi–Dirac distribution function**:

$$f_{\boldsymbol{k}}^0 = \frac{1}{\exp[(E_{\boldsymbol{k}} - \mu_{\mathrm{F}})/(k_{\mathrm{B}}T)] + 1}, \tag{5.14}$$

where μ_{F} is the chemical potential (also called Fermi energy when $T \approx 0$) and k_{B} the Boltzmann constant. The equation governing the variation of $f_{\boldsymbol{k}}$ in the presence of an external perturbation is known as the **Boltzmann equation**:

$$\frac{df_{\boldsymbol{k}}}{dt} = \left(\frac{\partial f_{\boldsymbol{k}}}{\partial t}\right)_{\text{field}} + \left(\frac{\partial f_{\boldsymbol{k}}}{\partial t}\right)_{\text{diff}} + \left(\frac{\partial f_{\boldsymbol{k}}}{\partial t}\right)_{\text{scatt}}. \tag{5.15}$$

Equation (5.15) includes the effects on $f_{\boldsymbol{k}}$ due to the applied field, the diffusion of carriers, and the scattering of carriers by phonons, impurities, etc. For simplicity, we shall assume that the diffusion term is negligible and the applied field $\boldsymbol{F}$ is small enough that we can expand $f_{\boldsymbol{k}}$ about $f_{\boldsymbol{k}}^0$ as a function of $\boldsymbol{F}$:

$$f_{\boldsymbol{k}} = f_{\boldsymbol{k}}^0 + g_{\boldsymbol{k}}(\boldsymbol{F}). \tag{5.16}$$

With this approximation we can write $(\partial f_{\boldsymbol{k}}/\partial t)_{\text{field}}$ as

$$\left(\frac{\partial f_{\boldsymbol{k}}}{\partial t}\right)_{\text{field}} \approx \left(\frac{\partial f_{\boldsymbol{k}}^0}{\partial E_{\boldsymbol{k}}}\right)\left(\frac{dE_{\boldsymbol{k}}}{dt}\right) = \left(\frac{\partial f_{\boldsymbol{k}}^0}{\partial E_{\boldsymbol{k}}}\right) q\boldsymbol{v}_{\boldsymbol{k}} \cdot \boldsymbol{F}, \tag{5.17}$$

where $\boldsymbol{v}_{\boldsymbol{k}}$ is the velocity of carriers with wave vector $\boldsymbol{k}$. Within the **relaxation time approximation**, we assume that the net effect of the scattering processes is to cause $g_{\boldsymbol{k}}$ to relax with a time constant $\tau_{\boldsymbol{k}}$, so that

$$\left(\frac{\partial f_{\boldsymbol{k}}}{\partial t}\right)_{\text{scatt}} \approx -\frac{g_{\boldsymbol{k}}}{\tau_{\boldsymbol{k}}}. \tag{5.18}$$

At steady state $df_{\boldsymbol{k}}/dt = 0$, and after substituting (5.17) and (5.18) into (5.15) we obtain

$$g_{\boldsymbol{k}} = \left(\frac{\partial f_{\boldsymbol{k}}^0}{\partial E_{\boldsymbol{k}}}\right) q\tau_{\boldsymbol{k}}\boldsymbol{v}_{\boldsymbol{k}} \cdot \boldsymbol{F}. \tag{5.19}$$

The corresponding generalized expression for the current density is now given by

$$\boldsymbol{j} = \int q f_{\boldsymbol{k}} \boldsymbol{v}_{\boldsymbol{k}} d\boldsymbol{k} = \int q g_{\boldsymbol{k}} \boldsymbol{v}_{\boldsymbol{k}} d\boldsymbol{k} \tag{5.20}$$

$$= q^2 \int \tau_{\boldsymbol{k}} \boldsymbol{v}_{\boldsymbol{k}} \left(\frac{\partial f^0_{\boldsymbol{k}}}{\partial E_{\boldsymbol{k}}}\right) (\boldsymbol{v}_{\boldsymbol{k}} \cdot \boldsymbol{F}) d\boldsymbol{k}, \tag{5.21}$$

since $\int q f^0_{\boldsymbol{k}} \boldsymbol{v}_{\boldsymbol{k}} d\boldsymbol{k} = 0$. Using (5.21) the corresponding expressions for σ and μ can be easily obtained.

5.2.2 Nondegenerate Electron Gas in a Parabolic Band

As an example of how to apply (5.21) we will consider the simple case of a nondegenerate electron gas in a parabolic band with an isotropic effective mass m^* in a cubic crystal. In such crystal $\boldsymbol{j}$ and $\boldsymbol{v}_{\boldsymbol{k}}$ are parallel to $\boldsymbol{F}$, at least in the region where Ohm's law holds. The distribution function (5.14) for a nondegenerate electron gas can be approximated by the **Boltzmann distribution**:

$$f^0_{\boldsymbol{k}} \propto \exp\left[-E_{\boldsymbol{k}}/(k_{\mathrm{B}}T)\right] \tag{5.22}$$

so that

$$\frac{\partial f^0_{\boldsymbol{k}}}{\partial E_{\boldsymbol{k}}} \propto -\frac{1}{k_{\mathrm{B}}T} \exp\left(\frac{-E_{\boldsymbol{k}}}{k_{\mathrm{B}}T}\right). \tag{5.23}$$

The integration over $\boldsymbol{k}$-space in (5.21) can be replaced by an integration over the energy $E_{\boldsymbol{k}}$ using the density of states (DOS) introduced in Sect. 4.3.1. For a parabolic band in three dimensions, the DOS $D(E)$ is given by (including spin degeneracy):

$$D(E) = \frac{1}{\pi^2} k^2 \frac{dk}{dE} = \frac{1}{2\pi^2} \left(\frac{2m^*}{\hbar^2}\right)^{3/2} E^{1/2}. \tag{5.24}$$

Substituting these results into (5.21) we can calculate j and hence σ:

$$\sigma = \left(\frac{q^2}{3\pi^2 m^* k_{\mathrm{B}}T}\right) \left(\frac{2m^*}{\hbar}\right)^{3/2} \int_0^\infty \tau(E) E^{3/2} \exp\left(-E/(k_{\mathrm{B}}T)\right) dE. \tag{5.25}$$

In analogy with (5.10) we can define an **average scattering time** $\langle\tau\rangle$ by

$$\sigma = \frac{1}{m^*} \int_0^\infty D(E) q^2 \langle\tau\rangle dE. \tag{5.26}$$

Comparing (5.25) and (5.26) we obtain

$$\langle\tau\rangle = \left(\frac{2}{3k_{\mathrm{B}}T}\right) \frac{\int_0^\infty \tau(E) E^{3/2} \exp\left[-E/(k_{\mathrm{B}}T)\right] dE}{\int_0^\infty E^{1/2} \exp\left[-E/(k_{\mathrm{B}}T)\right] dE}. \tag{5.27}$$

Using $\langle\tau\rangle$ we can express the mobility for a nondegenerate electron gas as

$$\mu = q\langle\tau\rangle/m^*. \tag{5.28}$$

From the expression for $\langle\tau\rangle$ we notice that the mobility depends on the electron temperature T. In order to calculate this temperature dependence, it is necessary to know the dependence of the scattering mechanisms on electron energy.

5.2.3 Dependence of Scattering and Relaxation Times on Electron Energy

Carriers in a semiconductor are scattered by their interaction with the following excitations [Ref. 5.2, pp. 82–183]:

- phonons: both acoustic and optical,
- ionized impurities,
- neutral defects,
- surfaces and interfaces,
- other carriers (e. g., scattering between electrons and holes).

In order to calculate the relaxation time $\tau_{\boldsymbol{k}}$ to be used in (5.18), we have to first consider the effect of scattering on $f_{\boldsymbol{k}}$. Let us define $P(\boldsymbol{k},\boldsymbol{k}')$ as the probability per unit time that an electron with wave vector $\boldsymbol{k}$ will be scattered into another state $\boldsymbol{k}'$. Once this scattering rate is known the rate of change of $f_{\boldsymbol{k}}$ caused by scattering can be calculated with the equation

$$\left(\frac{\partial f_{\boldsymbol{k}}}{\partial t}\right)_{\text{scatt}} = \sum_{\boldsymbol{k}'\neq\boldsymbol{k}} \left[P(\boldsymbol{k}',\boldsymbol{k})f_{\boldsymbol{k}'}(1-f_{\boldsymbol{k}}) - P(\boldsymbol{k},\boldsymbol{k}')f_{\boldsymbol{k}}(1-f_{\boldsymbol{k}'})\right]. \tag{5.29}$$

The first term inside the square brackets represents the rate at which an electron at $\boldsymbol{k}'$ will be scattered into the state at $\boldsymbol{k}$, while the second term is the rate for scattering out of the state $\boldsymbol{k}$ into $\boldsymbol{k}'$. The summation is over all processes which conserve both energy and wave vector. If we assume as before that the electron gas is nondegenerate, then $f_{\boldsymbol{k}}$ and $f_{\boldsymbol{k}'}$ are small and can be neglected compared with unity. Applying the **principle of detailed balance**, $P(\boldsymbol{k}',\boldsymbol{k})f^0_{\boldsymbol{k}'} = P(\boldsymbol{k},\boldsymbol{k}')f^0_{\boldsymbol{k}}$, see [5.3], (5.29) simplifies to

$$-\left(\frac{\partial f_{\boldsymbol{k}}}{\partial t}\right)_{\text{scatt}} = \sum_{\boldsymbol{k}'\neq\boldsymbol{k}} P(\boldsymbol{k},\boldsymbol{k}')\left[f_{\boldsymbol{k}} - (f_{\boldsymbol{k}'}f^0_{\boldsymbol{k}}/f^0_{\boldsymbol{k}'})\right]. \tag{5.30}$$

In general, $(\partial f_{\boldsymbol{k}}/\partial t)_{\text{scatt}}$ *cannot* be expressed as $-(f_{\boldsymbol{k}} - f^0_{\boldsymbol{k}})/\tau_{\boldsymbol{k}}$ as assumed in the relaxation time approximation. Only with more assumptions do we obtain an expression of the form (Problem 5.2)

$$\left(\frac{\partial f_{\boldsymbol{k}}}{\partial t}\right)_{\text{scatt}} = -(f_{\boldsymbol{k}} - f^0_{\boldsymbol{k}})\left(\sum_{\boldsymbol{k}'\neq\boldsymbol{k}} P(\boldsymbol{k},\boldsymbol{k}')\right), \tag{5.31}$$

from which a scattering time τ_{s} can be defined as

$$(1/\tau_{\mathrm{s}}) = \sum_{\boldsymbol{k}'\neq\boldsymbol{k}} P(\boldsymbol{k},\boldsymbol{k}'), \tag{5.32}$$

where the summation is over all the final states $\boldsymbol{k}'$ that satisfy both energy and momentum conservation. However, τ_s represents the residence time of the electron in state $\boldsymbol{k}$ before being scattered and is not the same as $\tau_{\boldsymbol{k}}$, which is equal to the time it takes a perturbed distribution to return to equilibrium. In order for thermal equilibrium to be achieved, carriers have to be scattered in and out of a state many times. When $P(\boldsymbol{k}, \boldsymbol{k}')$ is known, it is possible to calculate $\tau_{\boldsymbol{k}}$ numerically by following the time evolution of the distribution function of an electron gas using a Monte Carlo simulation technique [5.4, 5].

5.2.4 Momentum Relaxation Times

We shall now obtain analytical expressions for $\tau_{\boldsymbol{k}}$ by making some approximations. One approach is to equate $\tau_{\boldsymbol{k}}$ to a **momentum relaxation time** τ_m. We can argue that the most important effect of scattering on electron transport is the randomization of the electron velocity. The relevant quantity is a **momentum relaxation rate** defined by

$$\langle d\boldsymbol{k}/dt \rangle = \boldsymbol{k}(\tau_m)^{-1} = \sum_{\boldsymbol{k}' \neq \boldsymbol{k}} (\boldsymbol{k}' - \boldsymbol{k}) P(\boldsymbol{k}, \boldsymbol{k}'). \tag{5.33}$$

The scattering rate $P(\boldsymbol{k}, \boldsymbol{k}')$ can be calculated using Fermi's Golden Rule

$$P(\boldsymbol{k}, \boldsymbol{k}') = (2\pi/\hbar) |\langle \boldsymbol{k} \,|\, H_{\text{scatt}} \,|\, \boldsymbol{k}' \rangle|^2 \varrho_f, \tag{5.34}$$

where H_{scatt} is the Hamiltonian for the scattering processes which conserve both energy and wave vector, and ϱ_f is the density of final states $\boldsymbol{k}'$ per unit volume of crystal. Of the scattering processes listed earlier, the ones most effective in randomizing the electron momentum are those with impurities and with phonons. Scattering by the *static* potential of impurities is elastic. Scattering by *acoustic* phonons is nearly elastic (quasi-elastic) because of the small energy transfers involved; the average scattering angles are large. As we saw in Chap. 3, optical phonons in semiconductors have energies in the range of tens of meV, therefore scattering between electrons and optical phonons is inelastic.

We will now calculate the individual rates for these scattering processes. Afterwards these rates can be *added* together to calculate the total scattering rate whose inverse is a measure of the relaxation time.

a) Intraband Scattering by Acoustic Phonons

We will assume that an electron with initial energy E_k and wave vector $\boldsymbol{k}$ is scattered to another state with energy $E_{k'}$ and wave vector $\boldsymbol{k}'$ via the emission of an acoustic phonon with energy E_p and wave vector $\boldsymbol{q}$. Since the total energy and wave vector of the electron and phonon have to be conserved in the scattering in a periodic lattice, the initial and final electron energies and wave vectors are related by the equations (for the case of phonon emission)

$$E_{k'} - E_k = E_p \quad \text{and} \quad \boldsymbol{k}' - \boldsymbol{k} = \boldsymbol{q}. \tag{5.35}$$

For an acoustic phonon with a small $\boldsymbol{q}$, E_p is related to $\boldsymbol{q}$ by

$$E_p = \hbar v_s q, \tag{5.36}$$

where v_s is the phonon velocity. For simplicity we shall assume v_s to be isotropic.

We shall further assume that the electron is in a parabolic band with effective mass m^* and it is scattered by acoustic phonons within the same band (this is known as **intraband scattering**). Since the scattering process conserves energy and wave vector, the allowed values of $\boldsymbol{q}$ are obtained by combining (5.35) and (5.36) into

$$(\hbar^2/2m^*)(k^2 - |\boldsymbol{k} - \boldsymbol{q}|^2) = \hbar v_s q \tag{5.37}$$

and solving for $\boldsymbol{q}$. The final electronic states, after emission of an acoustic phonon, are shown schematically in Fig. 5.1a. From this picture it is clear that the allowed values of q lie between a minimum (q_{min}) and a maximum (q_{max}). For $k > mv_s/\hbar$, q_{min} is zero while q_{max} is reached when $\boldsymbol{k}'$ is diagonally opposite to $\boldsymbol{k}$, i. e., when the electron is scattered by 180° (backscattering). From (5.37) q_{max} can easily be calculated to be

$$q_{max} = 2k - (2mv_s/\hbar). \tag{5.38}$$

The energy lost by the electron in emitting this phonon is

$$E_k - E_{k'} = \hbar v_s q_{max} = 2\hbar v_s k - 2mv_s^2. \tag{5.39}$$

To estimate the order of magnitude of these quantities, we will assume the following values of the parameters involved: $m^* = 0.1m_0$ (m_0 is the free electron mass), $v_s = 10^6$ cm/s, and $E_k = 25$ meV (roughly corresponding to room temperature times k_B). For this electron $k = 2.6 \times 10^6\ \mathrm{cm}^{-1}$, $q_{max} = 5 \times 10^6\ \mathrm{cm}^{-1} \approx 2k$, $k' = 2.4 \times 10^6\ \mathrm{cm}^{-1}$ ($\boldsymbol{k}' \approx -\boldsymbol{k}$) and $E_k - E_{k'} = 3.3$ meV. In emitting an acoustic phonon with wave vector $\boldsymbol{q}_{max}$, the electron completely

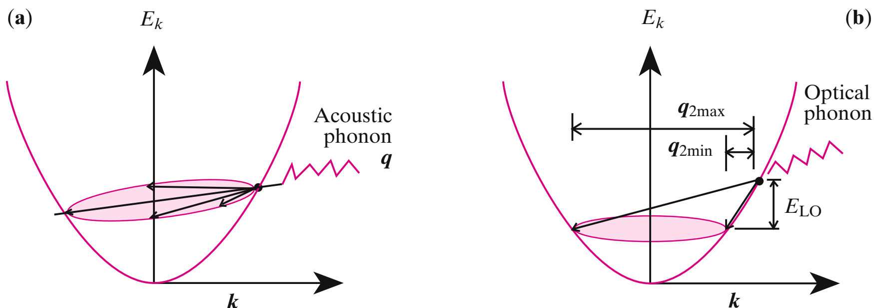

Fig. 5.1. Schematic diagrams for the scattering of an electron in a parabolic band by emission of (**a**) an acoustic phonon and (**b**) a longitudinal optical (LO) phonon showing the final electronic states and also the range of phonon wave vectors allowed by wave vector conservation

reverses its direction but its energy changes by only about 13 %. Thus scattering between electrons and acoustic phonons is nearly elastic (or quasi-elastic) and the main effect of these collisions is the relaxation of electron momentum.

Using (5.34) we shall now calculate the probability $P_{LA}(\boldsymbol{k},\boldsymbol{q})$ that an electron in a parabolic and nondegenerate band will emit a LA phonon of wave vector $\boldsymbol{q}$. First we shall consider only the *deformation potential mechanism* and use the electron LA–phonon interaction Hamiltonian H_{e-LA} defined in (3.21 and 22). The scattering matrix element in (5.34) will now be written as $|\langle \boldsymbol{k},N_{\boldsymbol{q}}\,|\,H_{e-LA}\,|\,\boldsymbol{k}',N'_{\boldsymbol{q}}\rangle|^2$, where $|\,\boldsymbol{k},N_{\boldsymbol{q}}\rangle$ represents the initial state with the electron in state $\boldsymbol{k}$ and the occupation number (for a definition see Sect. 3.3.1, p. 126) of LA phonons with wave vector $\boldsymbol{q}$ equal to $N_{\boldsymbol{q}}$. Similarly, $|\,\boldsymbol{k}',N'_{\boldsymbol{q}}\rangle$ is the final state, where the phonon occupation number is changed to $N'_{\boldsymbol{q}}$ and the electron is scattered to state $\boldsymbol{k}'$. We will be interested in one-phonon scattering only, i. e., $N'_{\boldsymbol{q}}$ differs from $N_{\boldsymbol{q}}$ by ± 1. Since our goal here is to calculate the temperature dependence of the electron mobility with (5.27), we are concerned only with the dependence of P_{LA} on electron energy and temperature. As discussed already in Sect. 3.3.1, we can express $|\langle \boldsymbol{k},N_{\boldsymbol{q}}\,|\,H_{e-LA}\,|\,\boldsymbol{k}',N'_{\boldsymbol{q}}\rangle|^2$ as

$$|\langle \boldsymbol{k},N_{\boldsymbol{q}}\,|\,H_{e-LA}\,|\,\boldsymbol{k}',N'_{\boldsymbol{q}}\rangle|^2 \propto q\left(N_{\boldsymbol{q}}+\tfrac{1}{2}\pm\tfrac{1}{2}\right), \tag{5.40}$$

where the $+(-)$ sign in (5.40) corresponds to emission (absorption) of a phonon by the electron. As also shown in Sect. 3.3.1, $N_{\boldsymbol{q}}$ at room temperature can be approximated by $k_B T/(\hbar v_s q) \gg 1$, so that $|\langle \boldsymbol{k},N_{\boldsymbol{q}}\,|\,H_{e-LA}\,|\,\boldsymbol{k}',N'_{\boldsymbol{q}}\rangle|^2$ is proportional to $N_{\boldsymbol{q}} \gg 1$ for both phonon emission and absorption. As a result, we can deduce the following dependence of P_{LA} on T and E_k

$$P_{LA}(\boldsymbol{k}) = \sum_{q} P_{LA}(\boldsymbol{k},\boldsymbol{q}) \propto \int q N_q \delta[E_k - E_{k'} - \hbar v_s q]d\boldsymbol{q}. \tag{5.41}$$

Using polar coordinates, (5.41) can be expressed as

$$P_{LA}(\boldsymbol{k}) \propto \int_0^{q_{max}} q^3 (T/q)dq \int_0^{\pi} \delta\left\{\left[\hbar^2 q/(2m)\right](2k\cos\Theta + q) - \hbar v_s q\right\} d(\cos\Theta) \tag{5.42a}$$

$$\approx T q_{max}^2 / k, \tag{5.42b}$$

where Θ is the angle between $\boldsymbol{k}$ and $\boldsymbol{q}$. Since q_{max} is approximately equal to $2k$, P_{LA} is roughly proportional to kT. Thus the P_{LA} produced by the deformation potential mechanism depends on the electron energy $E_{\boldsymbol{k}}$ and temperature as (see Problem 5.3)

$$P_{LA} \propto T(E_k)^{1/2}. \tag{5.43}$$

In noncentrosymmetric crystals, carriers can be scattered by both LA and TA phonons via the piezoelectric interaction (Sect. 3.3.3). Again we are interested mainly in the energy dependence of the corresponding scattering matrix element: $|\langle \boldsymbol{k},N_{\boldsymbol{q}}\,|\,H_{pe}\,|\,\boldsymbol{k}',N'_{\boldsymbol{q}}\rangle|^2$. From (3.30) and (3.22) we obtain

$$|\langle \boldsymbol{k},N_{\boldsymbol{q}}\,|\,H_{pe}\,|\,\boldsymbol{k}',N'_{\boldsymbol{q}}\rangle|^2 \propto (1/q)\left(N_{\boldsymbol{q}}+\tfrac{1}{2}\pm\tfrac{1}{2}\right). \tag{5.44}$$

Unlike $|\langle \boldsymbol{k}, N_{\boldsymbol{q}} \,|\, H_{\mathrm{e-LA}} \,|\, \boldsymbol{k}', N'_{\boldsymbol{q}} \rangle|^2$, the constant of proportionality in (5.44) depends, in general, on the direction of $\boldsymbol{q}$, so we cannot simply substitute (5.44) into (5.41) to calculate the electron–phonon scattering rate due to the piezoelectric interaction. However, by comparing the dependence on q in (5.44 and 40) it is clear that the piezoelectric interaction is more important for small-q phonons. Since phonons with small q are less effective in relaxing carrier momentum, we may argue that the piezoelectric interaction is less important than the deformation potential interaction in momentum relaxation. This is only true if the electromechanical constants are small, such as for semiconductors with low ionicity. In more ionic crystals, such as II–VI compound semiconductors, the piezoelectric interaction tends to dominate over the deformation potential interaction [5.6]. If we can assume the constant of proportionality in (5.44) to be independent of the direction of $\boldsymbol{q}$, then it is straightforward to show (Problem 5.4) that the piezoelectric electron–acoustic-phonon scattering rate P_{pe} is proportional to

$$P_{\mathrm{pe}} \propto T(E_k)^{-1/2}. \tag{5.45}$$

This expression is obviously not valid for very low energy electrons. When E_k is small, the wave vector q of the acoustic phonons involved in the scattering will be small also. Usually, in the case under consideration, corresponding to (5.45), free carriers are also present in the semiconductor, and therefore the macroscopic piezoelectric field associated with these long-wavelength phonons will be screened by the free carriers. For a nondengenerate electron gas this screening effect can be included by introducing a **screening wave vector** q_0, which is defined as the reciprocal of the **Debye screening length** λ_{D}, see [Refs. 5.1, p. 151; 5.2, p. 179; 6.10, p. 497]

$$q_0^2 = \frac{1}{\lambda_{\mathrm{D}}^2} = \frac{4\pi N e^2}{4\pi\varepsilon_0 \varepsilon_{\mathrm{s}} k_{\mathrm{B}} T}, \tag{5.46}$$

where ε_{s} is the static dielectric constant. The result is that the matrix element $|\langle \boldsymbol{k}, N_{\boldsymbol{q}} \,|\, H_{\mathrm{pe}} \,|\, \boldsymbol{k}', N'_{\boldsymbol{q}} \rangle|^2$ in (5.44) should be replaced by

$$|\langle \boldsymbol{k}, N_{\boldsymbol{q}} \,|\, H_{\mathrm{pe}} \,|\, \boldsymbol{k}', N'_{\boldsymbol{q}} \rangle|^2 \propto \left(\frac{q^3}{(q^2 + q_0^2)^2} \right) (N_{\boldsymbol{q}} + \tfrac{1}{2} \pm \tfrac{1}{2}). \tag{5.47}$$

Notice that (5.44) is recovered if $q_0 = 0$. When the screening effect is included in (5.47), i. e., $q_0 \neq 0$, $|\langle \boldsymbol{k}, N_{\boldsymbol{q}} \,|\, H_{\mathrm{pe}} \,|\, \boldsymbol{k}', N'_{\boldsymbol{q}} \rangle|^2$ approaches zero as $q \to 0$. Similarly P_{pe} goes to zero, rather than diverging like in (5.45), as the electron energy decreases to zero. Figure 5.2 shows qualitatively the dependence of P_{pe} on electron energy.

From (5.41) we see that carriers are more likely to be scattered by LA phonons with large q via the deformation potential interaction. Since these phonons are more effective in randomizing the carrier momentum, acoustic phonon scattering (via the deformation potential interaction) is the dominant mechanism for momentum relaxation of carriers at room or lower temperatures in most semiconductors except for the very ionic ones. The acoustic

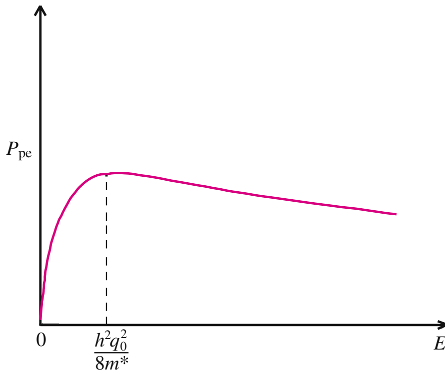

Fig. 5.2. Sketch of the dependence on the energy of an electron of the rate of scattering (P_{pe}) by acoustic phonons via the piezoelectric electron–phonon interaction [Ref. 5.2, Fig. 3.20]

phonon scattering time for conduction electrons in GaAs (via deformation potential interaction only) has been calculated by *Conwell* and *Vassel* [5.8]. Their results are shown in Fig. 5.3. Notice that this scattering time is of the order of several picoseconds (one picosecond is equal to 10^{-12} s and abbreviated as ps) in GaAs (Problem 5.3), and notice also how it decreases with increasing electron energy as predicted by (5.43).

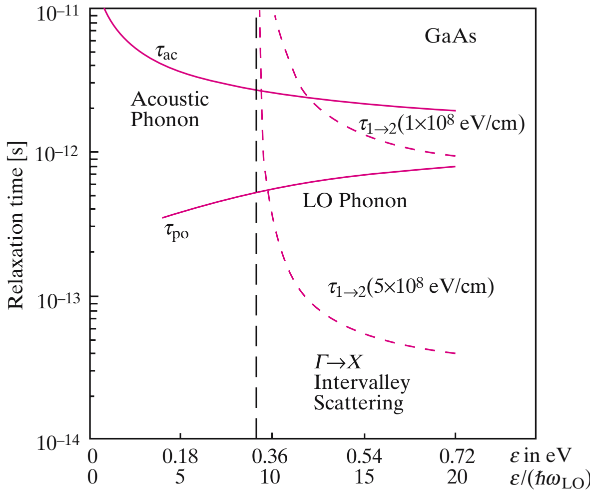

Fig. 5.3. Momentum relaxation times of a conduction electron in the Γ valley of GaAs as a function of electron energy. Scattering by: small wave vector LA phonons (τ_{ac}) via the deformation potential interaction; small wave vector optical phonons (τ_{po}) via the Fröhlich interaction and via zone-edge phonons from Γ to the X valleys ($\tau_{1\to2}$) calculated by *Conwell* and *Vassel* [5.8]. Notice that the deformation potential for the Γ to X intervalley scattering has been assumed to be either 1×10^8 or 5×10^8 eV/cm. These values are smaller than the now accepted value of 10^9 eV/cm [5.9]

b) Intraband Scattering by Polar Optical Phonons

Optical phonons in semiconductors typically have energies of the order of tens of meV (Chap. 3). Hence at low temperatures ($T < 100$ K) most electrons do not have sufficient energy to emit optical phonons. In addition, the thermal occupation number N_q of optical phonons is very low, and consequently the probability of an electron absorbing an optical phonon is small also. Thus, optical phonon scattering processes are negligible at low temperatures. On the other hand, at room temperature, where there are sufficient high-energy electrons to emit optical phonons, they tend to dominate over acoustic phonon scattering. This is particularly true in polar semiconductors, where the Fröhlich electron–phonon interaction (Sect. 3.3.5 and Fig. 5.3) can be very strong. The distribution of final electronic states after optical phonon scattering is shown schematically in Fig. 5.1b. While scattering by acoustic phonons relaxes mainly the electron momentum, scattering by optical phonons contributes to both momentum and energy relaxation.

The LO phonon scattering probability (P_{LO}) corresponding to $P_{\mathrm{LA}}(\boldsymbol{k})$ in (5.42) can be shown to be [Ref. 5.2, p. 115, 5.10]

$$P_{\mathrm{LO}} \propto \int_0^\infty \left(\frac{q^2}{(q^2+q_0^2)^2}\right) q^2 dq \int_0^\pi d(\cos\Theta)\big\{N_{\mathrm{LO}}\delta[E_{k'}-(E_k+E_{\mathrm{LO}})] + (N_{\mathrm{LO}}+1)\delta[E_{k'}-(E_k-E_{\mathrm{LO}})]\big\}, \tag{5.48}$$

where N_{LO} and E_{LO} are, respectively, the LO phonon occupation number and energy. For simplicity we have assumed that the LO phonon is dispersionless, which is usually a good approximation since only phonons with $q \lesssim q_0$ contribute significantly to (5.48). The term inside the first set of parentheses comes from the Fröhlich matrix element, including screening. The terms proportional to N_{LO} and $N_{\mathrm{LO}}+1$ are identified with phonon absorption and emission, respectively. As a result of wavevector conservation in (5.35), (5.48) can be expressed as

$$P_{\mathrm{LO}} \propto \int_0^\infty \left(\frac{q^4}{(q^2+q_0^2)^2}\right) dq \int_0^\pi \left\{N_{\mathrm{LO}}\delta\left[\left(\frac{\hbar^2 q}{2m}\right)(k\cos\Theta+q)-E_{\mathrm{LO}}\right] +(N_{\mathrm{LO}}+1)\delta\left[\left(\frac{\hbar^2 q}{2m}\right)(-k\cos\Theta+q)+E_{\mathrm{LO}}\right]\right\} d(\cos\Theta). \tag{5.49}$$

Integrating over Θ results in the following expression for P_{LO}:

$$P_{\mathrm{LO}} \propto N_{\mathrm{LO}} \int_{q_{1\,\mathrm{min}}}^{q_{1\,\mathrm{max}}} \left(\frac{q^3}{(q^2+q_0^2)^2}\right) dq + (N_{\mathrm{LO}}+1) \int_{q_{2\,\mathrm{min}}}^{q_{2\,\mathrm{max}}} \left(\frac{q^3}{(q^2+q_0^2)^2}\right) dq, \tag{5.50}$$

where $q_{i\,\mathrm{max}}$ and $q_{i\,\mathrm{min}}$ are, respectively, the maximum and minumum values of the LO phonon wave vector for phonon absorption ($i = 1$) and phonon emission ($i = 2$) (Problem 5.5). From Fig. 5.1b one can easily identify the

electron final states corresponding to the minumum and maximum values of q. Since $q_{i\,\min}$ is nonzero for optical phonons, the screening wave vector in (5.50) is not as important as for piezoelectric acoustic phonons, except in the case of highly doped semiconductors. If we neglect q_0 in (5.50), P_{LO} decreases as $1/q$ and scattering by small-q LO phonons is more likely than by large-q LO phonons. In contrast to the case of acoustic phonon scattering, scattering between electrons and LO phonons tends to relax the electron energy rather than its momentum.

The momentum relaxation time of an electron due to LO phonon scattering can be deduced from (5.50) using (5.33). The result is [Ref. 5.2, p. 118]

$$\begin{aligned}\left(\frac{1}{\tau_{\mathrm{m}}}\right) \propto\; & N_{\mathrm{LO}}\left(\frac{E_k+E_{\mathrm{LO}}}{E_k}\right)^{1/2}+(N_{\mathrm{LO}}+1)\left(\frac{E_k-E_{\mathrm{LO}}}{E_k}\right)^{1/2}\\ & +\left(\frac{E_{\mathrm{LO}}}{E_k}\right)\left[-N_{\mathrm{LO}}\sinh^{-1}\left(\frac{E_k}{E_{\mathrm{LO}}}\right)^{1/2}\right.\\ & \left.+(N_{\mathrm{LO}}+1)\sinh^{-1}\left(\frac{E_k-E_{\mathrm{LO}}}{E_{\mathrm{LO}}}\right)^{1/2}\right]. \qquad (5.51)\end{aligned}$$

A plot of the relaxation time for electrons in GaAs due to LO phonon scattering (via the Fröhlich interaction) is shown in Fig. 5.3 under the label τ_{po}. Typically the relaxation time due to scattering by LO phonons is less than 1 ps.

c) Intervalley Scattering

The role of intervalley scattering in electron relaxation is different in direct and indirect bandgap semiconductors. In direct bandgap semiconductors, such as GaAs and InP, intervalley scattering is important only for electrons with sufficient energy to scatter into the higher conduction band valleys. Since these valleys are several tenths of an eV above the conduction band minimum at zone center, in these semiconductors *intervalley* scattering is important only for their hot electron transport properties. This will be discussed in more detail in Sect. 5.4. The situation is quite different in indirect bandgap semiconductors, such as Si and Ge. In these materials the electrons are located in conduction band minima which are not at zone center and are degenerate. In addition to *intraband* scattering by phonons, electrons can be scattered from one degenerate valley to another via intervalley scattering. In both materials the latter scattering processes turn out to be more important than the intraband processes in relaxing the momentum and energy of conduction electrons. In this section we shall consider only intervalley scattering of electrons in indirect bandgap semiconductors.

As an example, we discuss the case of Si, where the conduction band minima occur along the six equivalent [100] directions (Δ_1) at about 0.83 of the distance from zone center to the zone edge. Electrons in one of the minima (say in the [100] direction) can be scattered either into the valley along the [$\bar{1}$00] direction or into one of the four equivalent [0,$\pm$1,0] and [0,0,$\pm$1] valleys (Fig. 5.4a). The former process is known as a **g-process** and the phonon involved is known as a **g-phonon** while the latter processes are called

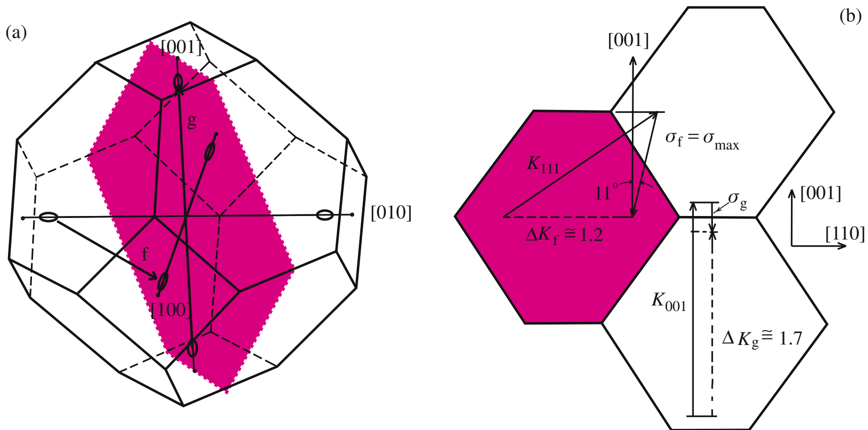

Fig. 5.4a,b. Schematic diagram of the intervalley scattering processes for electrons in the conduction band minimum of Si showing the phonon wave vectors involved in the g- and f-processes [Refs. 5.2 (Fig. 3.16), 5.11]. ΔK is given in units of $(2\pi/a_0)$.

f-processes. For both processes the electron valley after scattering can lie in the same Brillouin zone or in an adjacent one (Fig. 5.4b). The former process is known as a **normal process**, the latter as an **umklapp process** [Ref. 5.7, p. 146]. As shown in Fig. 5.4b, the wave vector $\Delta \boldsymbol{K}_g$ (note that, in order to show both the g- and f-phonons in this figure, the g-phonon is now chosen along the [001] direction) of the phonon mediating the normal g-process is about 1.7 times the Brillouin zone length along the X axis. On the other hand, the phonon wave vector ($\boldsymbol{\sigma}_g$) of the umklapp g-process is only ≈ 0.34 of the Brillouin zone edge (measured from the zone center) in the $[00\bar{1}]$ direction. The reciprocal lattice vector involved in the g umklapp process, denoted by $\boldsymbol{K}_{001}$, is also along the X direction. The f-phonon $\Delta \boldsymbol{K}_f$ is approximately equal to 1.2 times $(2\pi/a_0)(1, \pm 1, 0)$, a_0 being the size of the unit cube in Si. The wave vector lies outside the first Brillouin zone. Hence both g- and f-processes require phonons with wave vectors outside the first Brillouin zone. Thus in the reduced zone scheme only umklapp processes are allowed. Combined with a reciprocal lattice vector $\boldsymbol{K}_{111} = (2\pi/a_0)(1, 1, 1)$, the resultant umklapp wave vector $\boldsymbol{\sigma}_f$ is about 11° off the [001] direction (Σ_1 symmetry) with length almost exactly equal to that of the zone-boundary value along that direction (Fig. 5.4b). The symmetries and energies of intervalley phonon modes allowed by group theory in Si are (see Fig. 3.1 and [5.2], p. 110)

g-process: Δ_2' (LO), 63 meV

f-processes: Σ_1 (LA, TO; 45 and 57 meV; an average of 54 eV was used in [5.2], p. 110).

The corresponding selection rules for intervalley scattering in III–V compounds have been derived by *Birman* et al. [5.12].

In order to fit the temperature dependence of the mobility of Si it was found necessary to include a contribution to intervalley scattering from a phonon of 16 meV energy [5.11]. According to the phonon dispersion curves

of Si, this 16 meV phonon (Fig. 3.1; 16 meV $\Leftrightarrow$ 130 cm^{-1} $\Leftrightarrow$ 3.9 THz) can be attributed to an LA mode with wave vector about 0.3 times the zone boundary, corresponding to the g umklap process of Fig. 5.4. This process is strictly speaking forbidden since the corresponding matrix element has $\Delta_1 \otimes \Delta_1 \otimes \Delta_{2'} = \Delta_{2'}$ symmetry and therefore vanishes. The presence of such processes, required by the first of the resistivity vs T curve has been explained by expanding the electron–phonon interaction as a function of phonon wave vector beyond the lowest (zeroth) order term [5.13]. Except for the higher order electron–phonon interactions, the calculation of the intervalley scattering rates is similar, in principle, to that for acoustic phonons in direct bandgap semiconductors. In practice the calculation is complicated by the anisotropy in the electron mass in Si. Assuming for the sake of simplicity an isotropic mass, we find that the intervalley scattering rate due to the zeroth-order electron–phonon interaction is given by

$$(1/\tau_{\mathrm{iv}}) \propto N_q(E_k + E_{\mathrm{p}})^{1/2} + (N_q + 1)(E_k - E_{\mathrm{p}})^{1/2} U(E_k - E_{\mathrm{p}}), \tag{5.52a}$$

where E_{p} is the phonon energy and $U(x)$ is the step function:

$$U(x) = \begin{cases} 0 & \text{for } x < 0, \\ 1 & \text{for } x \geq 0. \end{cases} \tag{5.52b}$$

Readers interested in the contribution to the scattering rate from the first-order electron–phonon interaction should consult either [5.13] or [Ref. 5.2, p. 110].

d) Scattering by Impurities

Typically a semiconductor contains defects such as impurities and dislocations. Carriers are scattered elastically by these defects, the details of the scattering mechanism depending on the defect involved. Here we will concern ourselves with scattering by the most common kind of defects, namely, charged impurities. Free carriers are produced in semiconductors by ionization of shallow impurities (except in the intrinsic case where they are produced by thermal ionization across the gap). As a result, free carriers will, in principle, always be scattered by the ionized impurities they leave behind. A way to avoid this will be presented in the next section.

Our approach to calculating impurity scattering rates will be different from the approach for phonon scattering. Phonons are quantized lattice waves with well-defined wave vectors and therefore they scatter electrons from one Bloch state to another. Impurity potentials are localized in space. Hence they do not scatter electrons into well-defined Bloch states. This problem can be treated quantum mechanically using scattering theory and what is referred to as the **Brooks–Herring approach** [Refs. 5.2, p. 143; 5.14]. In this approach the impurity potential is approximated by a screened Coulomb potential. The screening can be either Debye [with the screening length of (5.46)] or *Thomas–Fermi* [Ref. 5.7, p. 266]. The scattering cross section is calculated within the Born approximation. The quantum mechanical results obtained by *Brooks* [5.14] are not too different from the classical results obtained earlier by *Conwell* and *Weisskopf* [5.15] so we shall first consider the **Conwell–Weisskopf approach**.

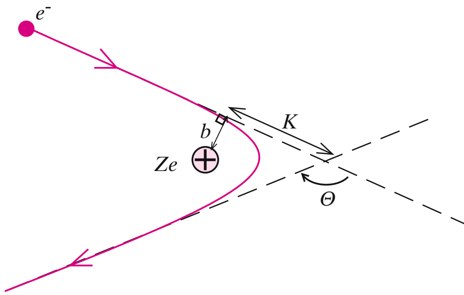

Fig. 5.5. Coulomb scattering of an electron by a positively charged ion. The impact parameter b and the length K are discussed in the text. [Ref. 5.2, Fig. 4.1]

Conwell–Weisskopf Approach. In this approach an electron is assumed to be scattered classically via Coulomb interaction by an impurity ion with charge $+Ze$. The corresponding scattering cross section is calculated in exactly the same way as for the Rutherford scattering of α particles [5.16]. The scattering geometry of this problem is shown schematically in Fig. 5.5. The *scattering cross section* σ as a function of the scattering angle Θ is given by

$$\sigma(\Theta)d\Omega = 2\pi b\, d\,|\,b\,| \tag{5.53}$$

where $d\Omega$ is an element of solid angle, b is known as the **impact parameter**. and $d\,|\,b\,|$ is the change in $|\,b\,|$ required to cover the solid angle $d\Omega$. The impact parameter and the solid angle $d\Omega$ are related to the scattering angle by

$$b = K\cot(\Theta/2);\;\; d\Omega = 2\pi\sin\Theta d\Theta \tag{5.54}$$

where K is a characteristic distance defined by

$$K = \frac{Ze^2}{mv_k^2} \tag{5.55}$$

and v_k is the velocity of an electron with energy $E_k = mv_k^2/2$. If $d\Omega$ and $d\,|\,b\,|$ are expressed in terms of $d\Theta$, (5.53) can be simplified to

$$\sigma(\Theta) = \left(\frac{K}{2\sin^2(\Theta/2)}\right)^2. \tag{5.56}$$

The well-known dependence of σ on the electron velocity to the power of -4 in Rutherford scattering is contained in the term K^2. The scattering rate R (per unit time) of particles traveling with velocity v by N scattering centers per unit volume, each with *scattering cross section* σ, is given by

$$R = N\sigma v. \tag{5.57}$$

Since scattering by impurities relaxes the momenta of carriers, but not their energy, we can define a momentum relaxation time $\tau_{\rm i}$ due to impurity scattering by

$$1/\tau_{\rm i} = N_{\rm i}v_k\int\sigma(\Theta)(1-\cos\Theta)2\pi\sin\Theta\, d\Theta, \tag{5.58}$$

where $N_{\rm i}$ is the concentration of ionized impurities. Within the integrand, the term $(1-\cos\Theta)$ is the fractional change in the electron momentum due to scattering event and the term $2\pi\sin\Theta\, d\Theta$ represents integration of the solid

angle Ω. In principle, Θ has to be integrated from 0 to π. The divergence of (5.56) at $\Theta = 0$ makes the integral in (5.58) diverge. This problem can be avoided by arguing that b cannot be larger than a maximum value $b_{\max}$ equal to half of the average separation between the ionized impurities:

$$b_{\max} = \tfrac{1}{2} N_i^{-1/3}. \tag{5.59}$$

As a result the minimum value of Θ allowable in (5.58) is

$$\Theta_m = 2\cot^{-1}(b_{\max}/K). \tag{5.60}$$

Integrating (5.58) with the condition (5.60) we obtain the following expression for $1/\tau_{\mathrm{i}}$:

$$1/\tau_{\mathrm{i}} = -4\pi N_{\mathrm{i}} v_k K^2 \ln[\sin(\Theta_m/2)] \tag{5.61}$$

or, in terms of the electron energy E_k,

$$\frac{1}{\tau_{\mathrm{i}}} = 2\pi N_{\mathrm{i}} \left(\frac{2E_k}{m}\right)^{1/2} \left(\frac{Ze^2}{2E_k}\right)^2 \ln\left[1 + \left(\frac{E_k}{N_{\mathrm{i}}^{1/3} Ze^2}\right)^2\right]. \tag{5.62}$$

The scattering rate of electrons by ionized impurities is independent of temperature and depends on the electron energy approximately like $E_k^{-3/2}$ due to the dependence of the scattering cross section on the particle velocity in (5.56). As a result, ionized impurity scattering tends to become dominant at low temperature where the electron energies are small and, moreover, phonon scattering freezes out.

Brooks–Herring Approach. As mentioned earlier, in the Brooks–Herring approach the scattering rate of electrons by ionized impurities is calculated quantum mechanically. If the effect of screening of the impurity potentials by free carriers is taken care of by introducing a screening wave vector q_0 [which is the reciprocal of the Debye screening length] defined in (5.46), then (5.56) must be replaced by

$$\sigma(\Theta) = \left[\frac{K}{2\sin^2\dfrac{\Theta}{2} + \left(\dfrac{q_0}{2k}\right)^2}\right]^2. \tag{5.63}$$

In this way the divergence in $\sigma(\Theta)$ at $\Theta = 0$ in (5.56) is automatically avoided without introducing, in a somewhat artificial way, the maximum impact parameter $b_{\max}$.

The electron mobility (assuming that the only scattering process is by ionized impurities) calculated by the Brooks–Herring approach (BH for short) is compared with that calculated by the Conwell-Weisskopf approach (curves labeled CW) in Fig. 5.6 as a function of carrier density for a hypothetical uncompensated semiconductor. Except for high carrier concentrations the two results are almost identical. However, for very high carrier concentrations even the Brooks–Herring approach breaks down. The question of screening at high carrier concentrations has been studied by many researchers and a detailed account can be found in [Ref. 5.2, pp. 145–152].

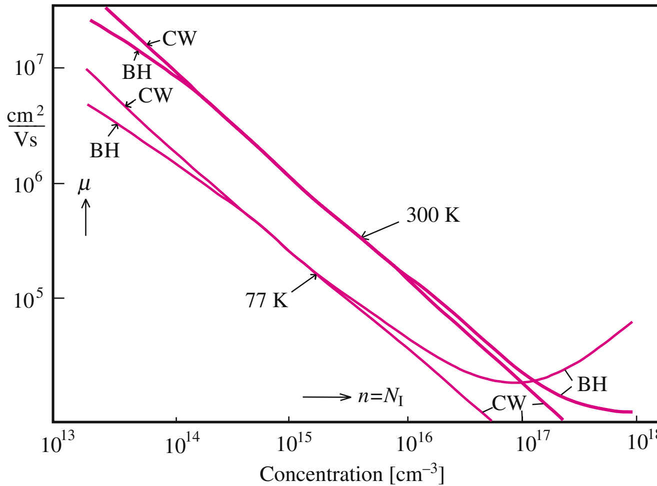

Fig. 5.6. Mobility of electrons calculated by considering only ionized impurity scattering as a function of impurity concentration. The curves labeled CW have been calculated classically by *Conwell* and *Weisskopf* [5.15]. The curves labeled BH have been calculated quantum mechanically using the Brooks–Herring approach [5.14]

5.2.5 Temperature Dependence of Mobilities

We are now in a position to discuss the temperature dependence of carrier mobilities in a nondegenerate semiconductor with parabolic bands. From the scattering rates of an electron in a band we first calculate the electron lifetime $\tau(E_k)$ by taking the reciprocal of the total scattering rate. Next we substitute $\tau(E_k)$ into (5.27) to obtain $\langle\tau\rangle$. Since the different scattering mechanisms have different dependences on electron energy and temperature, they result in different temperature dependences of the mobility. By comparing the measured temperature dependence of the mobility with theory one can determine the contributions from the different scattering mechanisms. To facilitate this comparison we note that if $\tau(E_k)$ can be expressed as a function of E_k and T as being proportional to E_k^n and T^m then

$$\int E^{3/2} \exp(-E/k_B T)\tau(E) dE \propto T^{m+n+5/2} \tag{5.64}$$

and

$$\langle\tau\rangle \propto T^{m+n}. \tag{5.65}$$

Using the energy and temperature dependence of the scattering rate obtained in the previous section we can conclude that

- $\mu \propto T^{-3/2}$ for acoustic phonon (deformation potential) scattering;
- $\mu \propto T^{-1/2}$ for acoustic phonon (piezoelectric) scattering;
- $\mu \propto T^{3/2}$ for ionized impurity scattering.

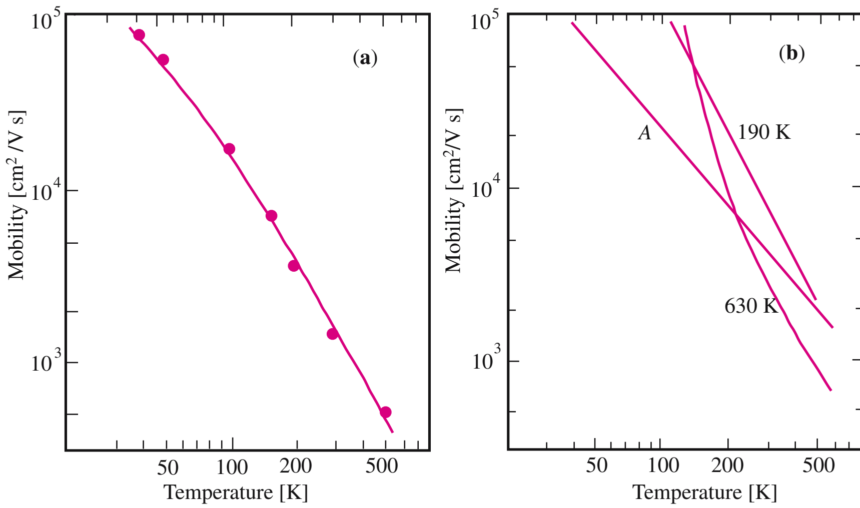

Fig. 5.7a,b. Temperature dependence of mobility in n-type Si. The *solid curve* in (**a**) represents the experimental results. The *curves* in (**b**) are the relative contributions to the mobility from scattering by different kinds of phonons. Curve *A* represents the contribution from *intravalley* acoustic phonon scattering while the other two curves represent contributions from *intervalley* scattering by phonons whose energies correspond to temperatures of 190 K (or 16 meV) and 630 K (54 meV). The *filled circles* in (**a**) display a fit to the experimental curve using the theoretical curves in (**b**) [5.13]

Figure 5.7 shows the temperature dependence of the mobility in intrinsic n-type Si. The experimental results [solid curve in (a)] can be explained by a combination of intravalley scattering by acoustic phonons and intervalley scattering by two phonons of energies 16 meV (129 cm^{-1}, TA) and 54 meV (436 cm^{-1}, LO). The electron–phonon interaction for the LO intervalley scattering is symmetry allowed for phonons along Δ while that for the TA phonon is forbidden. *Ferry* [5.13] attributed the nonvanishing value of the latter to contributions from phonons close to but not exactly along Δ.

Figure 5.8 shows the mobility in n-type Si for various donor concentrations. The shape of the experimental curves at high donor concentrations can be explained by the dominance of ionized impurity scattering at low temperatures, as sketched in the inset. The experimental temperature dependence of mobility in n-type GaAs is compared with theory in Fig. 5.9. Again the experimental results can be understood in terms of ionized impurity scattering at low temperatures and phonon scattering at higher temperatures. At room temperature, the scattering of electrons in GaAs is dominated by the polar LO phonon processes.

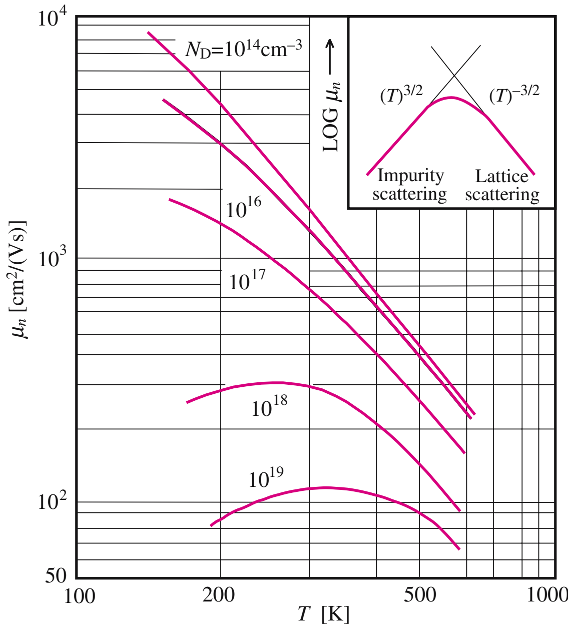

Fig. 5.8. Temperature dependence of mobilities in n-type Si for a series of samples with different electron concentrations. The inset sketches the temperature dependence due to lattice and impurity scattering [5.17]

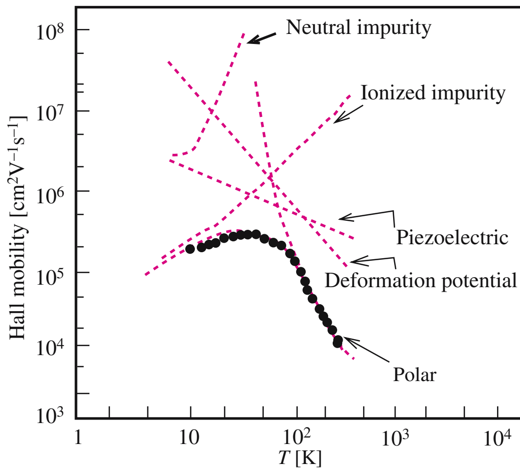

Fig. 5.9. Temperature dependence of mobility in n-type GaAs determined by Hall measurements (*points*) by *Stillman* et al. [5.18]. The dashed curves are the corresponding contributions from various scattering mechanisms calculated by *Fletcher* and *Butcher* [5.19] (from [5.19])

5.3 Modulation Doping

From the temperature dependence of mobilities in Si and GaAs we conclude that scattering by ionized impurities ultimately limits the carrier mobility at low temperatures. This limitation can be circumvented by using the method of **modulation doping** proposed by *Störmer* et al. [5.20].

The idea behind modulation doping is illustrated in Fig. 5.10. Two materials with almost identical lattice constants but different bandgaps are grown on top of each other to form a **heterojunction** (see Chap. 9). One example of a well-behaved heterojunction used commonly in the fabrication of semiconductor laser diodes is GaAs/$Al_xGa_{1-x}As$ (other examples will be discussed in Chap. 9). The lattice constants of these two semiconductors differ by less than 1 %. The bandgap of AlGaAs with less than 40 % of Al is direct and larger than that of GaAs. The difference between their bandgaps is divided in an approximately 60/40 split between the conduction and valence bands (for further discussions see Chap. 9). The results are very abrupt discontinuities, known as **band offsets**, in their energy bands at the interface, as shown schematically in Fig. 5.10. If the material with the larger bandgap (AlGaAs) is then doped with shallow donors, the Fermi level is shifted from the middle of the bandgap of AlGaAs to the donor level. In order to maintain a constant chemical potential throughout the two materials, electrons will flow from AlGaAs to GaAs. This causes the band edges to bend at the interface as shown in Fig. 5.10, a phenomenon known as **band bending**. We shall show in Sect. 8.3.3 that band bending also occurs near the surface of semiconductors as a result of the existence of surface states.

Due to band bending the electrons in GaAs are now confined by an approximately triangular potential near the interface and form a *two-dimensional (2D) electron gas*. These 2D electrons are physically separated from the ion-

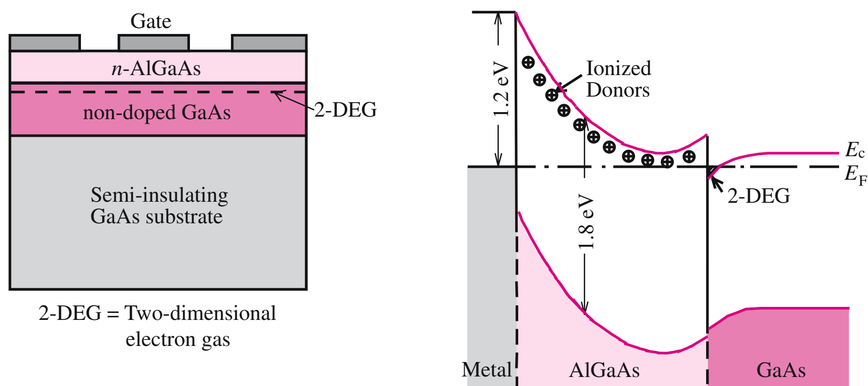

Fig. 5.10. The structure and band diagram of a modulation-doped heterojunction between GaAs and n-AlGaAs. E_c and E_F represent, respectively, the conduction band edge and the Fermi energy

ized impurities in AlGaAs, hence they are only weakly scattered by the charged impurities. This method constitutes the *modulation doping* technique mentioned above [5.20]. If scattering by interface defects can be avoided, the mobility of the 2D electron gas in a modulation-doped sample can approach the theoretical limit set by phonon scattering in the absence of impurity scattering. Using this method carrier mobilities exceeding 10^6 cm^2/(Vs) have been achieved in GaAs. Figure 5.11 shows the temperature dependence of the mobility of a 2D electron gas at a GaAs/$Al_{0.3}Ga_{0.7}As$ heterojunction. Notice that unlike the mobility depicted in Fig. 5.9, the mobility in Fig. 5.11 does not decrease when the temperature is lowered towards zero, as would be expected if scattering by ionized impurities were present. However, some residual scattering by the potential of the impurities located inside the $Al_{0.3}Ga_{0.7}As$ is still present; it is labeled "remote impurities" in Fig. 5.11. It approaches a small constant value at low temperatures so that modulation doping improves the carrier mobility when phonon scattering is frozen. Since electron scattering in these samples is dominated by phonons (except at very low temperatures), it is possible to determine the absolute volume deformation potentials of LA

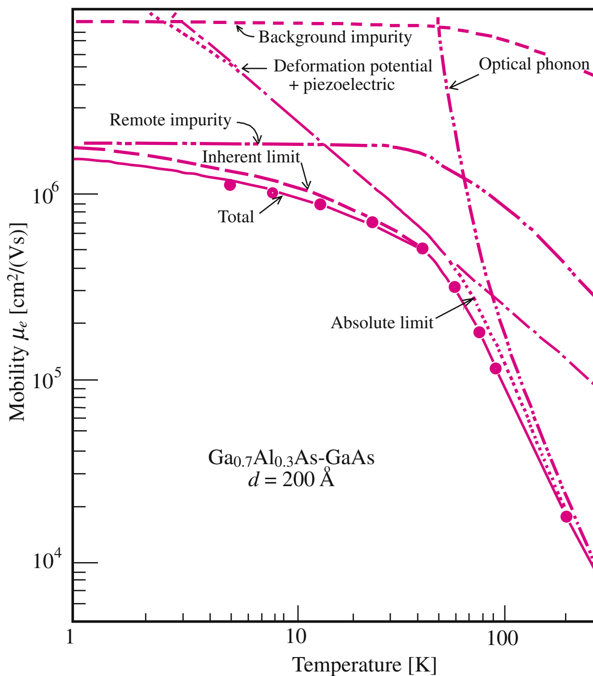

Fig. 5.11. Mobility of a two-dimensional electron gas in a modulation-doped GaAs/$Ga_{0.7}Al_{0.3}As$ heterojunction as a function of temperature. The closed circles indicate the experimental results. The various *broken curves* represent calculated contributions to the mobility from different scattering mechanisms. The *solid curve* represents the sum of all those contributions [5.21]

phonons quite accurately from the temperature dependence of the electron mobility [5.21].

Modulation doping is now utilized in the fabrication of field-effect transistors with very high mobility. These transistors are known either as **MODFET**s (which stands for *modulation-doped field-effect transistors*) or **HEMT**s (*high electron mobility transistors*) [Ref. 5.22, p. 698].

5.4 High-Field Transport and Hot Carrier Effects

The formalism developed in Sect. 5.1 for calculating the carrier drift velocity leads to Ohm's law and is valid only at low electric fields. In most semiconductors we find that Ohm's law breaks down at electric fields exceeding 10^4 V/cm. In this section we shall study the effect of high electric fields on carrier distributions and also other transport phenomena which can occur under high electric fields. As we pointed out in the introduction, these high-field effects can only be calculated numerically [5.4, 5.23] and therefore our discussions will necessarily be qualitative.

The main difficulty in these calculations results from the very fast rates at which carriers gain energy under the high electric field. When these rates are larger than those for energy loss to the lattice, the carriers are no longer at thermal equilibrium with the lattice. There are two possible scenarios for these nonequilibrium situations. In one case, carriers are in thermal equilbrium among themselves but not with the phonons. In this situation carriers can be said to be in **quasi thermal equilibrium**. Their distribution can still be characterized by a Fermi–Dirac distribution, albeit with a temperature different from the *sample temperature* (defined as that of the phonons which are in equilibrium with the thermal sink to which the sample is attached). Usually these carriers have higher temperatures than the lattice, hence they are known as **hot carriers**. In the second scenario, the carriers cannot be described by an equilibrium distribution and therefore do not have a well-defined temperature. In the literature one may also find that these nonthermal equilibrium carriers are loosely referred to as hot carriers. More precisely these carriers should be called **nonequilibrium carriers**. Hot-carrier effects are important in the operation of many semiconductors devices such as *laser diodes*, *Gunn oscillators*, and *short-channel field-effect transistors* [Ref. 5.22, pp. 698–720]. The hot carriers in these devices are generated electrically by a high field or by injection through a barrier. Hot carriers can also be produced optically by high intensity photon beams such as in *laser annealing* [5.24].

What conditions determine whether a carrier distribution is an equilibrium one or not? The answer depends on the magnitude of the various time scales which characterize the interaction among the carriers and their interaction with the lattice relative to the carrier lifetime. Let us define the time it takes a nonequilibrium carrier distribution to relax to equilibrium as the **thermal-**

ization time. Processes contributing to thermalization are carrier–carrier and carrier–phonon interactions. As shown in Fig. 5.3, carrier–phonon interaction times can range from 0.1 ps (for polar optical phonons and for phonons in intervalley scattering) to tens of picoseconds (for acoustic phonons). Carrier–carrier interaction times depend strongly on carrier density. This has been measured optically in GaAs. At high densities ($>10^{18}$ cm^{-3}) carriers thermalize in times as short as *femtoseconds* (equal to 10^{-15} s and abbreviated as fs) [5.25]. Thus the thermalization time is determined by carrier–carrier interaction at high carrier densities. At low densities, it is of the order of the shortest carrier–phonon interaction time. Often carriers have a finite lifetime because they can be trapped by defects. If both electrons and holes are present, the carrier lifetime is limited by **recombination** (Chap. 7). In samples with a very high density of defects (such as amorphous semiconductors) carrier lifetimes can be picoseconds or less. Since the carrier lifetime determines the amount of time carriers have to thermalize, a distribution is a nonequilibrium one when the carrier lifetime is shorter than the thermalization time. A transient nonequilibrium situation can also be created by perturbing a carrier distribution with a disturbance which lasts for less than the thermalization time.

The properties of hot carriers can be different from those of equilibrium carriers. One example of this difference is the dependence of the drift velocity on electric field. Figure 5.12 shows the drift velocity in Si and GaAs as a function of electric field. At fields below 10^3 V/cm, the carriers obey Ohm's law, namely, the drift velocity increases linearly with the electric field. At higher fields the carrier velocity increases sublinearly with field and saturates at a velocity of about 10^7 cm/s. This leveling off of the carrier drift velocity at high field is known as **velocity saturation**. n-Type GaAs shows a more complicated behavior in that its velocity has a maximum *above* the saturation velocity. This phenomenon is known as **velocity overshoot** (Fig. 5.12) and is found usually only in a few n-type semiconductors such as GaAs, InP, and InGaAs. For

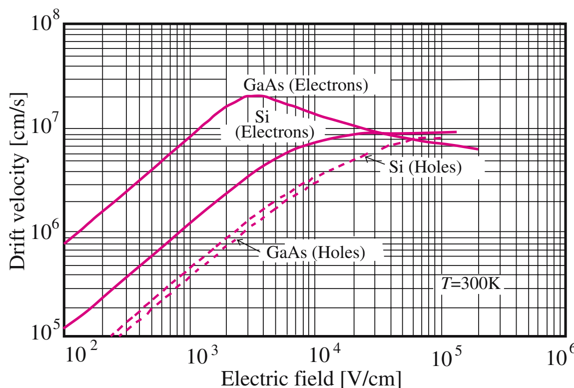

Fig. 5.12. Dependence of drift velocity on electric field for electrons and holes in Si and GaAs [5.17]. Notice the velocity overshoot for electrons in GaAs

electric fields between 3×10^3 V/cm and 2×10^5 V/cm, the velocity of electrons in GaAs *decreases* with increasing electric field. This phenomenon is known as **negative differential resistivity**. We shall consider these high field behaviors of carriers separately.

5.4.1 Velocity Saturation

The Boltzmann equation (5.15) is difficult to solve under high-field conditions, for which the carrier distribution can be a nonequilibrium one. One simplifying approach is to expand the carrier distribution as a function of carrier velocity in a Taylor series. This leads to a field-dependent mobility of the form

$$\mu(F) = \mu(0) + \beta F^2 + \dots \, . \tag{5.66}$$

Carriers are sometimes referred to as **warm carriers** when only the terms up to βF^2 are important [Ref. 5.26, p. 102]. As mentioned in Sect. 5.1, hot carrier properties are usually calculated numerically using a Monte Carlo simulation method; a discussion of these calculations is beyond the scope of this book [5.27]. Instead, we will present a highly simplified explanation of why the drift velocity in most semiconductors saturates at more or less the same value of 10^7 cm/s.

Within the quasi-classical approach that we adopted in Sect. 5.1, carriers in a semiconductor are regarded as free particles with effective mass m^*. Their average energy $\langle E \rangle$ can be defined as $\langle E \rangle = m^* v_d^2/2$, where v_d is their drift velocity. The saturation in v_d under a high electric field therefore implies that the average energy of the carriers no longer increases with electric field at high field strengths. This can be understood if there is an energy loss mechanism that becomes dominant at large $\langle E \rangle$. Scattering with optical phonons is the most obvious candidate. A simple-minded picture of what happens is as follows. At low fields, carriers are scattered elastically by acoustic phonons and these processes lead to momentum relaxation of the carriers. The carrier distribution is essentially a “drifted” equilibrium distribution (Problem 5.2). At intermediate fields, $\langle E \rangle$ becomes large enough for some of the carriers in the high-energy tail of the distribution to start to scatter *inelastically* with optical phonons. This distorts the carrier distribution and causes $\langle E \rangle$ to increase sublinearly with the field. At still higher fields, more of the carriers are scattered inelastically, until energy relaxation processes dominate. When the rate at which carriers gain energy from the field is balanced exactly by the rate of energy loss via optical phonon emission, $\langle E \rangle$ (and also v_d) becomes independent of electric field.

The saturation velocity v_s can thus be deduced from the energy-loss rate equation

$$\frac{d\langle E \rangle}{dt} = eFv_s - \frac{E_{op}}{\tau_e}, \tag{5.67}$$

where E_{op} is the optical phonon energy and τ_e is the energy relaxation time. A corresponding rate equation for momentum relaxation is

$$\frac{d(m^* v_s)}{dt} = eF - \frac{m^* v_s}{\tau_m}, \tag{5.68}$$

where τ_m is the momentum relaxation time. Assuming that scattering by optical phonons is the dominant process at high fields, both τ_e and τ_m are equal to the optical phonon scattering time τ_{op}. In the steady state, $d\langle E\rangle/dt = 0$ and $d(m^* v_s)/dt = 0$. Therefore the solution for v_s from (5.67) and (5.68) is simply

$$v_s = (E_{op}/m^*)^{1/2}. \tag{5.69}$$

Notice that τ_{op} is absent in the expression for v_s. For most tetrahedrally bonded semiconductors, the optical phonon energy is of the order of 40 meV and the carrier effective mass m^* is of the order of $0.1m_0$. Substituting these values into (5.69) we obtain $v_s \approx 2 \times 10^7$ cm/s. This explains both the constancy and order of magnitude of the experimental saturation velocities in many semiconductors.

5.4.2 Negative Differential Resistance

Electrical resistance is normally associated with dissipation of electrical energy in the form of heat in a conductor. Thus a negative electrical resistance suggests that electrical energy can be "created" in such a medium. However, it should be noted that a negative *differential* resistance (often abbreviated as NDR) is only a negative AC resistance. This means that NDR can be used in designing an AC amplifier only. When we study electronics we learn that an amplifier coupled with a properly designed positive feedback circuit can be made into an oscillator. Thus one important application of materials exhibiting NDR is in the construction of high-frequency (typically microwave frequencies) oscillators. The **Esaki tunnel diode**[1] is an example of a device exhibiting NDR [Ref. 5.22, pp. 641–643]. More recently **resonant tunneling diodes** (see Chap. 9 for further discussions) have also been shown to exhibit NDR [5.28]. The principles behind the NDR in these devices are different from those of n-type GaAs under a high electric field.

To understand the NDR in GaAs we have to refer to the conduction band structure shown in Fig. 2.14. While the lowest conduction band minimum in GaAs occurs at the Brillouin zone center, there are also conduction band minima at the L points, which lie about 0.3 eV higher in energy. The effective mass of electrons in these L valleys is not isotropic. For motion along the axis of the valleys, the longitudinal mass is $1.9m_0$ while the transverse mass is $0.075m_0$ [5.29]. These masses are much larger than the effective mass (to be denoted by m^*_Γ) of $0.067m_0$ for electrons in the Γ valley. On the basis of (5.12) we expect the mobility of electrons in the Γ valley (to be denoted by μ_Γ) to be larger than that of electrons in the L valleys (denoted by μ_L). At low electric fields all the electrons are in the Γ valley and the electron mobility is high

[1] Leo Esaki shared the 1973 Nobel Prize in Physics for his discovery of the phenomenon of electron tunneling in the diodes named after him.

because of the small m^*_Γ. As the field is increased, electrons gain energy until some of them have sufficient energy to transfer via intervalley scattering to the L valleys. This intervalley scattering now competes with intravalley relaxation via scattering by optical phonons. In GaAs the time it takes an electron to emit a LO phonon via the Fröhlich interaction (Fig. 5.3) is about 200 fs. The corresponding Γ to L intervalley scattering time at room temperature is less than 100 fs [5.30, 31]. However, the time it takes the electron to return to the Γ valley is of the order of picoseconds because the density of states of the Γ valley is much smaller than that of L valleys. As a result, for high enough electrics fields, we expect that a significant fraction of the electrons will be excited into the L valleys and the electron conductivity will become

$$\sigma = e(N_\Gamma \mu_\Gamma + N_L \mu_L), \tag{5.70}$$

where N_Γ and N_L are, respectively, the number of electrons in the Γ and L valleys. Since μ_L is smaller than μ_Γ, the conductivity decreases with increasing field, leading to a negative differential resistance. The field dependence of the electron drift velocity in GaAs deduced from the above picture is shown in Fig. 5.13. At even higher fields ($E > E_b$ in Fig. 5.13) there will be more electrons in the L valleys than in the Γ valley because the former have larger density of states and the intervalley transfer of electron stops. Now the electrons in the L valleys are accelerated by the external field and their velocities increase linearly with field again as shown schematically in Fig. 5.13. The threshold field E_c at which the drift velocity begins to decrease is commonly referred to as the **critical field**. It should be noted that at one time it was thought that the NDR in GaAs was caused by transfer of electrons to the X valleys. After it was demonstrated that the L valleys were lower in energy than the X valleys [5.32], transfer to the L valleys became accepted as the mechanism responsible for NDR in GaAs.

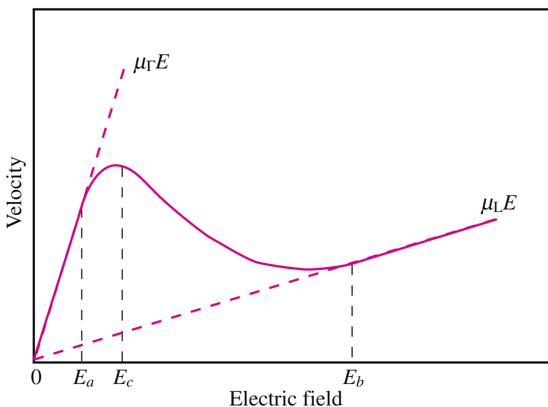

Fig. 5.13. Sketch of the dependence of the drift velocity of electrons in GaAs on electric field based on the qualitative model in Sect. 5.4.2

In order to observe NDR it is necessary to satisfy the following conditions. There must be higher energy valleys to which carriers can be excited under high electric field. The mobility of carriers in these higher energy valleys should be much smaller than in the lower energy valleys. The separation of the higher energy valleys from the lower energy valleys should be much larger than $k_B T$, where T is the device operation temperature, in order that the higher valleys are not populated thermally. However, this separation should not be larger than the bandgap. Otherwise, before the carriers have acquired enough energy from the field to transfer to the higher valleys they can already excite carriers from the valence band into the conduction band via **impact ionization** [Ref. 5.22, pp. 322–384]. These conditions are satisfied by the conduction bands of GaAs, InP [5.26], and the ternary alloy $In_xGa_{1-x}As$ ($x < 0.5$).

5.4.3 Gunn Effect

In 1963 *J. B. Gunn* [5.33, 34] discovered that when a thin sample (thickness of the order 10 μm) of n-type GaAs is subjected to a high voltage (such that the electric field exceeds the critical field E_c in GaAs), the current through the sample spontaneously breaks up into oscillations at microwave frequencies as shown in Fig. 5.14. The frequency of oscillation is inversely proportional to the length of the sample across which the field is applied. As will be shown below, the frequency of oscillation turns out to be equal to the saturation velocity v_s divided by the sample length. For sample lengths of the order of 10 μm and

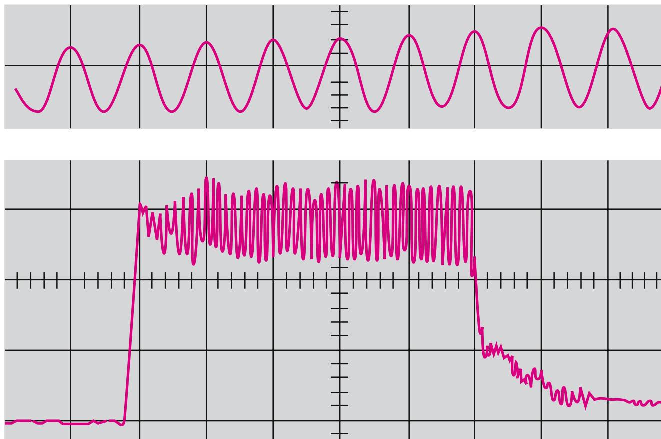

Fig. 5.14. Oscilloscope traces of Gunn oscillations in a thin piece of GaAs under a high electric field. Current waveform produced by the application of a voltage pulse of 16 V amplitude and 10 ns duration to a specimen of n-type GaAs 2.5×10^{-3} cm in length. The frequency of the oscillating component is 4.5 GHz. *Lower trace*: 2 ns/cm horizontally, 0.23 A/cm vertically. *Upper trace*: expanded view of lower trace [5.33]

v_s equal to 10^7 cm/s, the oscillation frequency is of the order of 10^{10} Hz, i. e. 10 gigahertz[2]. Electromagnetic waves of such high frequencies are known as **microwaves**. Hence the obvious application of the Gunn effect is the fabrication of microwave generators known as **Gunn diodes**.

The Gunn effect is one example of how NDR can lead to high-frequency oscillations. To understand this effect qualitatively [5.35], we will assume that the field dependence of the drift velocity in n-type GaAs has the simple form shown schematically in Fig. 5.15a. Suppose a constant high voltage is applied to the sample so that carriers drift from the left to right as shown schematically in Fig. 5.15b. We assume that the electric field is maintained at a value slightly below the threshold field E_c. Due to fluctuations in the electric field at finite temperatures, a small region labeled D in Fig. 5.15b has a field slightly above E_c at time $t = 0$. The carriers on both sides of D have now higher drift velocities than carriers inside D. As a result, carriers will pile up on the left hand side in D while the carrier density will drop on its right hand side. This charge pile-up in D at $t > 0$ leads to an increase in electric field inside D and a decreasing field outside, as shown in Fig. 5.15b. Because of the NDR for

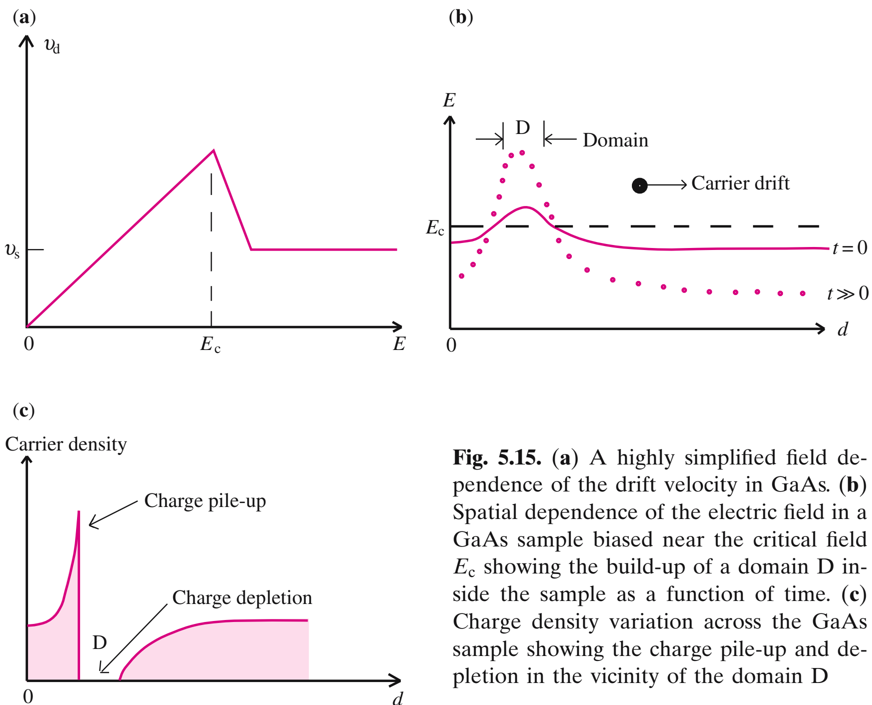

Fig. 5.15. (**a**) A highly simplified field dependence of the drift velocity in GaAs. (**b**) Spatial dependence of the electric field in a GaAs sample biased near the critical field E_c showing the build-up of a domain D inside the sample as a function of time. (**c**) Charge density variation across the GaAs sample showing the charge pile-up and depletion in the vicinity of the domain D

[2] The unit of frequency is hertz (Hz), named after Heinrich Hertz who produced and detected radio waves in 1888. One hertz is equal to one cycle per second.

fields larger than E_c, the increase in the field inside D leads to further slowing down of electrons inside D and hence more charge pile-up. This process, once started, will continue until most of the applied field is across D, as shown in the dotted curve in Fig. 5.15b for $t \gg 0$. Figure 5.15c displays the charge distribution along the length of the sample. The region D where the electric field is high is known as a **domain**. Only one domain can exist inside the sample at one time since most of the applied voltage will be across this domain. The most likely place for domains to be formed is the cathode, since the field fluctuations tend to be largest there. Under the influence of the applied voltage this domain will drift across the sample with the saturation velocity until it reaches the anode, thus giving rise to a periodic oscillation in current. The frequency of this oscillation is equal to v_s divided by the length of the sample. As a result of this oscillatory current, electromagnetic waves are radiated from the sample. From this simple description it is clear that Gunn oscillators are very efficient, yet miniature, microwave generators.

5.5 Magneto-Transport and the Hall Effect

We conclude this chapter by discussing the electric current induced in a sample in the presence of both electric and magnetic fields. As we pointed out in Sect. 5.1, in a cubic crystal the second-rank conductivity tensor $\boldsymbol{\sigma}$ can usually be represented by a diagonal matrix. This is not true when a magnetic field is present. In this case the conductivity tensor contains off-diagonal elements that are linearly dependent on the magnetic field. In this section we will derive this magneto-conductivity tensor and use the result to study an important phenomenon known as the Hall effect. Our approach in this section will be classical, leaving a quantum mechanical treatment to Chap. 9, where we shall consider the quantum Hall effect in two-dimensional electron gases.

5.5.1 Magneto-Conductivity Tensor

We shall first assume that the sample is an infinite, cubic and nonmagnetic crystal. Without loss of generality we can suppose that a magnetic field B_z is applied to the sample along the z axis, while an electric field $\boldsymbol{F}$ is applied along any arbitrary direction. To calculate the resultant current we use the quasi-classical approach adopted in Sect. 5.1. In the presence of both electric and magnetic fields, the equation of motion for the electrons (5.4) is replaced by the **Lorentz equation**:*

$$m^* \frac{d^2\boldsymbol{r}}{dt^2} + \frac{m^*}{\tau}\frac{d\boldsymbol{r}}{dt} = (-e)\left[\boldsymbol{F} + (\boldsymbol{v} \times \boldsymbol{B}/c)\right], \tag{5.71}$$

* The equations in this section are transformed into SI units by deleting the velocity of light c.

where c is the speed of light in vacuum. In (5.71) we have assumed that m^* and τ are isotropic. For generalizations see [5.36, 37]. Under steady-state conditions, $d\boldsymbol{v}/dt = d^2\boldsymbol{r}/dt^2 = 0$, we obtain

$$(m^*/\tau)\boldsymbol{v}_\mathrm{d} = (-e)\left[\boldsymbol{F} + (\boldsymbol{v}_\mathrm{d} \times \boldsymbol{B}/c)\right] \tag{5.72}$$

for the electron drift velocity $\boldsymbol{v}_\mathrm{d}$. In terms of its components along the x, y, and z axes, the three components of this equation can be written as

$$(m^*/\tau)v_{\mathrm{d},x} = (-e)\left[F_x + (v_{\mathrm{d},y}B_z/c)\right], \tag{5.73a}$$

$$(m^*/\tau)v_{\mathrm{d},y} = (-e)\left[F_y - (v_{\mathrm{d},x}B_z/c)\right], \tag{5.73b}$$

$$(m^*/\tau)v_{\mathrm{d},z} = (-e)F_z. \tag{5.73c}$$

By multiplying each of the above equations by the electron density n and charge $(-e)$ we obtain the corresponding equations for the current density $\boldsymbol{j} = n(-e)\boldsymbol{v}_\mathrm{d}$:

$$j_x = (ne^2\tau/m^*)F_x - (eB_z/m^*c)\tau j_y, \tag{5.74a}$$

$$j_y = (ne^2\tau/m^*)F_y + (eB_z/m^*c)\tau j_x, \tag{5.74b}$$

$$j_z = (ne^2\tau/m^*)F_z. \tag{5.74c}$$

It is convenient at this point to introduce the definitions

$$\sigma_0 = ne^2\tau/m^*, \tag{5.75}$$

which can be recognized as the zero-field conductivity, and

$$\omega_\mathrm{c} = eB_z/(m^*c), \tag{5.76}$$

which is the classical **cyclotron frequency** of the electron in the presence of the magnetic field B_z. Using these definitions, (5.74) can be simplified to

$$j_x = \sigma_0 F_x - \omega_\mathrm{c}\tau j_y, \tag{5.77a}$$
$$j_y = \sigma_0 F_y + \omega_\mathrm{c}\tau j_x, \tag{5.77b}$$
$$j_z = \sigma_0 F_z. \tag{5.77c}$$

Solving (5.77), we obtain the three components of the current density:

$$j_x = \frac{1}{1+(\omega_\mathrm{c}\tau)^2}\sigma_0(F_x - \omega_\mathrm{c}\tau F_y), \tag{5.78a}$$
$$j_y = \frac{1}{1+(\omega_\mathrm{c}\tau)^2}\sigma_0(F_y + \omega_\mathrm{c}\tau F_x), \tag{5.78b}$$
$$j_z = \sigma_0 F_z. \tag{5.78c}$$

Based on (5.78) we can define a generalized **magneto-conductivity tensor** $\boldsymbol{\sigma}(B)$ for the electrons as

$$\boldsymbol{\sigma} = \frac{\sigma_0}{1+(\omega_\mathrm{c}\tau)^2}\begin{pmatrix} 1 & -\omega_\mathrm{c}\tau & 0 \\ \omega_\mathrm{c}\tau & 1 & 0 \\ 0 & 0 & 1+(\omega_\mathrm{c}\tau)^2 \end{pmatrix}. \tag{5.79}$$

Notice that (5.79) contains the sum of a diagonal and an antisymmetric tensor. The sign of the off-diagonal elements depends on the sign of the charge.

From (5.79) we conclude that the effects of the magnetic field on the charge transport are twofold. (1) The conductivity perpendicular to the magnetic field is decreased by the factor $[1+(\omega_c\tau)^2]^{-1}$. The corresponding increase in the sample resistance induced by a magnetic field is known as **magnetoresistance** (for small values of B it is proportional to B^2). (2) The magnetic field also generates a current transverse to the applied electric field, resulting in off-diagonal elements in the conductivity tensor. These are linearly proportional to the magnetic field whereas the diagonal elements are quadratic in the magnetic field. The off-diagonal elements give rise to the Hall effect to be discussed in the next section.

5.5.2 Hall Effect

Let us consider a sample in the form of a rectangular bar oriented with its longest axis along the x axis, as shown in Fig. 5.16a. The electric field $\boldsymbol{F}$ is now applied along the x axis while the magnetic field $\boldsymbol{B}$ is still along the z axis. According to Lorentz's law, when electrons start to drift along the x axis under the influence of the electric field, they also experience a force in the y direction. This results in a current in the y direction although there is no applied electric field along that direction. One typical experimental configuration involves a closed current loop in the x direction while leaving an open circuit in

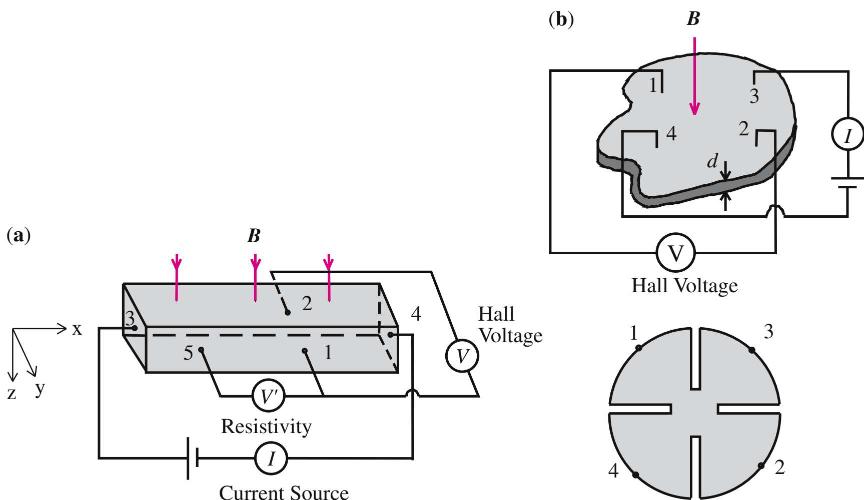

Fig. 5.16a, b. Sample geometries for performing Hall measurements: (**a**) sample in the form of a bar and (**b**) sample in the form of a thin film which is used in the van der Pauw method [5.39]. $\boldsymbol{B}$ denotes the magnetic field. I stands for the current source while V represents the meter for measuring the Hall voltage

the y direction, as shown in Fig. 5.16a. As a result of this open circuit the current density j_y must be zero. From (5.78b) we see that an electric field F_y is induced by the presence of the $\boldsymbol{B}$ field. This phenomenon is known as the **Hall effect** [5.38] after E.H. Hall (1855–1938), who discovered it at Johns Hopkins University in 1879 and then became a professor at Harvard [from 1881 to 1921].

A simple physical picture of what happens is as follows. The magnetic field causes the charges to drift in the y direction. As a result, charges pile up on the two opposite sample surfaces perpendicular to the y axis and create an electric field F_y, which cancels the effect of the Lorentz force. Under the steady-state condition $j_y = 0$, the induced field F_y is equal to

$$F_y = -\omega_c \tau j_x/\sigma_0 \tag{5.80a}$$

while the current measured in the x direction is given by

$$j_x = \sigma_0 F_x. \tag{5.80b}$$

The measured quantity in this experiment is F_y while the externally controlled parameters are j_x and $\boldsymbol{B}$. Therefore one defines the **Hall coefficient** R_H as the ratio

$$R_H = F_y/(j_x B_z). \tag{5.81}$$

Combining (5.80a) and (5.80b), we find that R_H is equal to[3]

$$R_H = -\frac{\omega_c \tau}{\sigma_0 B_z} = -\frac{1}{nec}. \tag{5.82}$$

Notice that the sign of R_H depends on the sign of the charge. While the Hall coefficient in (5.82) is negative (since we have assumed the charges are electrons), it can be easily shown that R_H becomes positive for holes. Thus we see that the Hall effect is an important technique for determining both the concentration and the sign of charged carriers in a sample. This technique is not limited to semiconductors only but is also used extensively in the study of metals. In compensated semiconductor samples, where both electrons and holes are present, R_H can be shown to be given by (Problem 5.6)

$$R_H = \frac{N_p - b^2 N_n}{ec(bN_n + N_p)^2}, \tag{5.83}$$

where N_n and N_p are the concentrations of the negative and positive charges, respectively, and b is the ratio of their mobilities: μ_n/μ_p. Corrections to (5.82) for the case of anisotropic masses and τ have been given by *Herring* and *Vogt* [5.37].

5.5.3 Hall Coefficient for Thin Film Samples (van der Pauw Method)

One limitation of the Hall effect measurement described in the previous section is the requirement that the sample be in the shape of a rectangular bar. As discussed in Sect. 1.2, samples are often grown in the form of thin epitaxial

[3] To convert to SI units delete c.

films on some insulating substrate. The extension of the Hall technique to such thin films was developed by *van der Pauw* [5.39]. Two common geometries for the van der Pauw method of measuring the Hall coefficient and resistivity in a thin sample are shown in Fig. 5.16b. This method is particularly convenient for a disk of irregular shape. The current is fed through the contacts 3 and 4 while the Hall voltage is measured across the contacts 1 and 2. The "clover" shape in Fig. 5.16b has the advantage of keeping the current flow away from the Hall voltage contacts. To minimize the error in the measurement of the Hall voltage due to the fact that the current flow may not be perpendicular to the line joining the contacts 1 and 2, one usually measures the voltage both with the magnetic field $V_{12}(\pm B)$ and without the field $V_{12}(0)$. Van der Pauw showed that the Hall coefficient is given by

$$R_{\mathrm{H}} = \frac{[V_{12}(B) - V_{12}(0)]d}{I_{34}B} = \frac{[V_{12}(B) - V_{12}(-B)]d}{2I_{34}B}, \tag{5.84}$$

where d is the thickness of the film, B is the magnetic field, and I_{34} is the current flowing from contact 3 to contact 4.

The sample resistivity ϱ can also be measured with the van der Pauw method. In this case two adjacent contacts such as 2 and 3 (I_{23}) are used as current contacts while the two remaining contacts are used for measuring the voltage drop (V_{41}). The resultant resistance is defined as $R_{41,23}$:

$$R_{41,23} = |V_{41}|/I_{23}. \tag{5.85}$$

Another measurement is then made in which current is instead sent through the contacts 1 and 3 and the voltage is measured across the contacts 2 and 4. From the resulting resistance $R_{24,13}$, together with $R_{41,23}$, ϱ can be calculated with the expression

$$\varrho = \frac{\pi d(R_{24,13} + R_{41,23})f}{2\ln 2} \tag{5.86}$$

where f is a factor that depends on the ratio $R_{24,13}/R_{41,23}$; f is equal to 1 when this ratio is exactly 1 [Ref. 5.26, p. 63]. When this ratio is equal to 10, f decreases to 0.7. Usually a large value for this ratio is undesirable and suggests that either the contacts are bad or that the sample is inhomogeneously doped.

5.5.4 Hall Effect for a Distribution of Electron Energies

So far we have assumed that all the charged carriers have the same properties. We shall now consider a collection of electrons with a range of energies E and a distribution function $f(E)$. We denote the average of any electron property $a(E)$ by $\langle a \rangle$:

$$\langle a \rangle = \int a(E)f(E)dE \Big/ \int f(E)dE. \tag{5.87}$$

Using this definition, (5.78) can be rewritten as

$$\langle j_x \rangle = \alpha F_x - \gamma B_z F_y \tag{5.88a}$$

$$\langle j_y \rangle = \alpha F_y + \gamma B_z F_x \tag{5.88b}$$
$$\langle j_z \rangle = \langle \sigma_0 \rangle F_x, \tag{5.88c}$$

where*

$$\alpha = \frac{ne^2}{m^*} \left\langle \frac{\tau}{1 + (\omega_c \tau)^2} \right\rangle \tag{5.89a}$$

$$\gamma = \frac{ne^3}{m^{*2}c} \left\langle \frac{\tau^2}{1 + (\omega_c \tau)^2} \right\rangle \tag{5.89b}$$

In the limit of a weak magnetic field or, when $(\omega_c\tau)^2 \ll 1$, we can approximate $1 + (\omega_c\tau)^2$ by one and thus write:

$$\alpha \simeq \frac{ne^2}{m^*}\langle\tau\rangle \quad \text{and} \quad \gamma \simeq \frac{ne^3\langle\tau^2\rangle}{m^{*2}c} \tag{5.90}$$

Within this approximation the Hall coefficient for a distribution of electrons can be expressed as[4]

$$R_H = \frac{\langle\tau^2\rangle}{(-nec)\langle\tau\rangle^2} = -\frac{r_H}{nec} \tag{5.91}$$

The factor $r_H = \langle\tau^2\rangle/\langle\tau\rangle^2$ is called the **Hall factor**. Its magnitude depends on the scattering mechanisms that contribute to τ and is usually of the order of 1 [Ref. 5.26, p. 57]. In the limit of strong magnetic fields, or for very pure samples, when $(\omega_c\tau)^2 \gg 1$, (5.91) remains valid with $r_H = 1$ (Problem 5.7). In principle we can determine the carrier mobility by measuring R_H and σ_0 and using (5.75 and 82) to obtain

$$\mu = R_H\sigma_0, \tag{5.92}$$

but in practice the carriers usually have a distribution of energies, so that the mobility calculated from (5.92) is not the same as the mobility μ defined by (5.12). Instead the mobility defined by (5.92) is referred to as the **Hall mobility** μ_H and is related to μ by

$$\mu_H = r_H\mu. \tag{5.93}$$

PROBLEMS

5.1 *Drifted Carrier Distributions*

Using (5.19) show that, within the relaxation time approximation, the carrier distribution in the presence of the field $\boldsymbol{F}$ can be approximated by

$$f_{\boldsymbol{k}} = f^0_{\boldsymbol{k}}(E_{\boldsymbol{k}} + q\tau_{\boldsymbol{k}}\boldsymbol{v}_{\boldsymbol{k}} \cdot \boldsymbol{F}).$$

for a small external field. This means that the effect of the electric field is to shift the entire distribution (without distortion) by the energy $q\tau_{\boldsymbol{k}}\boldsymbol{v}_{\boldsymbol{k}} \cdot \boldsymbol{F}$. This is just the energy gained by a charge q with velocity $\boldsymbol{v}_{\boldsymbol{k}}$ in the field $\boldsymbol{F}$ during a time $\tau_{\boldsymbol{k}}$.

[4] remove c to convert to SI units.

5.2 *a) Drifted Maxwell–Boltzmann Distributions*
Suppose the thermal equilibrium electron distribution $f_{\boldsymbol{k}}^0$ in (5.14) is approximated by a Boltzmann distribution function

$$f_{\boldsymbol{k}}^0 = A \exp\left[-E_{\boldsymbol{k}}/(k_{\mathrm{B}}T)\right].$$

For free carriers located in a spherical band with effective mass m^* the electron energy is given by $E_{\boldsymbol{k}} = (1/2)m^* v_{\boldsymbol{k}}^2$. The resultant $f_{\boldsymbol{k}}^0$ is known as a **Maxwell–Boltzmann distribution**. Using the result of Problem 5.1, show that the carrier distribution in the presence of a weak external electric field $\boldsymbol{F}$ can be approximated by

$$f_{\boldsymbol{k}} \approx A \exp\left(-\frac{m^*(\boldsymbol{v}_{\boldsymbol{k}} + \boldsymbol{v}_{\mathrm{d}})^2}{2k_{\mathrm{B}}T}\right),$$

where $\boldsymbol{v}_{\mathrm{d}}$ is the drift velocity defined in (5.6). The interpretation of this result is that the external field causes the carrier velocities to increase uniformly by an amount equal to $\boldsymbol{v}_d$ while leaving the distribution function unchanged. Consequently the resultant distribution is known as a **drifted Maxwell–Boltzmann distribution.**

b) Relaxation Time Approximation
The purpose of this problem is to show how the relaxation time approximation (5.18) can be obtained starting from (5.30). We will make the following assumptions:

1) The electronic band is isotropic, with effective mass m^*.
2) Scattering is completely elastic (so that $E_{\boldsymbol{k}'} = E_{\boldsymbol{k}}$ and $f_{\boldsymbol{k}}^0 = f_{\boldsymbol{k}'}^0$).
3) The applied field is weak so that (5.19) is valid.

a) With these assumptions, show that

$$f_{\boldsymbol{k}} - f_{\boldsymbol{k}'} = (f_{\boldsymbol{k}} - f_{\boldsymbol{k}}^0)\left[1 - (\boldsymbol{v}_{\boldsymbol{k}'} \cdot \boldsymbol{F})/(\boldsymbol{v}_{\boldsymbol{k}} \cdot \boldsymbol{F})\right].$$

Substitute this result into (5.30) and show that

$$\tau_{\boldsymbol{k}}^{-1} = \sum_{\boldsymbol{k}'} P(\boldsymbol{k}, \boldsymbol{k}')\left[1 - (\boldsymbol{v}_{\boldsymbol{k}'} \cdot \boldsymbol{F})/(\boldsymbol{v}_{\boldsymbol{k}} \cdot \boldsymbol{F})\right].$$

b) To simplify the above expression we choose (without loss of generality) coordinate axes such that $\boldsymbol{k}$ is parallel to the z-axis and $\boldsymbol{F}$ lies in the yz-plane. Let θ and θ' be, respectively, the angles between $\boldsymbol{k}$ and $\boldsymbol{F}$ and between $\boldsymbol{k}'$ and $\boldsymbol{F}$. Let the polar coordinates of $\boldsymbol{k}'$ in this system be (k', α, β). Show that

$$(\boldsymbol{v}_{\boldsymbol{k}'} \cdot \boldsymbol{F})/(\boldsymbol{v}_{\boldsymbol{k}} \cdot \boldsymbol{F}) = \tan\theta \, \sin\alpha \, \sin\beta + \cos\alpha.$$

c) Assume that the elastic scattering probability $P(\boldsymbol{k}, \boldsymbol{k}')$ depends on α but not on β. Show that

$$\tau_{\boldsymbol{k}}^{-1} = \sum_{\boldsymbol{k}'} P(\boldsymbol{k}, \boldsymbol{k}')(1 - \cos\alpha).$$

The physical interpretation of this result is that the relaxation time in elastic scattering is dominated by large angle scattering (i. e., processes with $\alpha \simeq \pi$).

5.3 *Intravalley Scattering by LA Phonons*
a) Using (5.42) show that the contribution of deformation potential interaction to the intravalley LA phonon scattering time (τ_{ac}) of an electron in a nondegenerate band with isotropic effective mass m^* and energy E is given by

$$\frac{1}{\tau_{ac}} = \frac{\sqrt{2}(a_c)^2(m^*)^{3/2}k_B T(E)^{1/2}}{\pi\hbar^4\varrho v_s^2},$$

where a_c is the volume deformation potential for the electron, T is the temperature, k_B is the Boltzmann constant, ϱ is the crystal density, and v_s is the LA phonon velocity.

b) Assume that the parameters in (a) have the following values, appropriate to GaAs: $m^* = 0.067$; $E = 0.36$ meV; $a_c = 6$ eV; $\varrho = 5.31$ g/cm^3, and $v_s = 5.22 \times 10^5$ cm/s. Show that $\tau_{ac} = 7 \times 10^{-12}$ s (7 ps) at $T = 300$ K.

5.4 *Piezoelectric Acoustic Phonon Scattering Rate*
Assume that the constant of proportionality in (5.44) is independent of angle. Substitute the result into (5.41) and perform the integration corresponding to that in (5.42). Show that instead of a scattering probability proportional to $T(E_k)^{1/2}$ as in (5.43), the probability for piezoelectric scattering is proportional to $T(E_k)^{-1/2}$. See p. 202 for discussions on how to remove the divergence in the scattering probability when $E_k \to 0$.

5.5 *Rate of Scattering by LO Phonons for Electrons in a Parabolic Band*
a) Consider a polar semiconductor with a dispersionless LO phonon energy $\hbar\omega_{LO}$. The Fröhlich electron–LO-phonon interaction Hamiltonian is given by (3.36). For an electron in a nondegenerate conduction band with isotropic effective mass m^*, the electron wave vector and energy above the band minimum are denoted by $\boldsymbol{k}$ and $E_{\boldsymbol{k}}$, respectively. Show that for $E_{\boldsymbol{k}} > \hbar\omega_{LO}$ the minimum and maximum phonon wave vectors, $q_{2\,\min}$ and $q_{2\,\max}$, of the phonon *emitted* by the electron are given by

$$q_{2\,\min} = k[1 - f(E_{\boldsymbol{k}})]$$

and

$$q_{2\,\max} = k[1 + f(E_{\boldsymbol{k}})]$$

where

$$f(E_{\boldsymbol{k}}) = \left[1 - (\hbar\omega_{LO}/E_{\boldsymbol{k}})\right]^{1/2}.$$

b) Show that the corresponding $q_{1\,\min}$ and $q_{1\,\max}$ for *absorption* of one LO phonon are given by

$$q_{1\,\min} = k[f'(E_{\boldsymbol{k}}) - 1]$$

and

$$q_{1\,\max} = k[f'(E_{\boldsymbol{k}}) + 1]$$

where

$$f'(E_{\boldsymbol{k}}) = \left[1 + (\hbar\omega_{\text{LO}}/E_{\boldsymbol{k}})\right]^{1/2}.$$

In the special case that $k = 0$,

$$q_{1\,\text{min}} = q_{1\,\text{max}} = [2m^* \omega_{\text{LO}}/\hbar]^{1/2}.$$

c) Substituting the above results into (5.50), show that the momentum relaxation rate by LO phonon scattering is given by (5.51) in the limit $q_0 = 0$.

d) Assume that a conduction band electron in GaAs has $E_{\boldsymbol{k}}/(\hbar\omega_{\text{LO}}) = 4$. Use the *Fröhlich* interaction in (3.36) to calculate the scattering rate of this electron by LO phonons. Some materials parameters for GaAs are: density $\varrho = 5.31$ g/cm^3; $m^* = 0.067 m_0$; $\varepsilon_0 = 12.5$; $\varepsilon_\infty = 10.9$; and $\hbar\omega_{\text{LO}} = 36$ meV.

5.6 *Hall Coefficient for Samples Containing both Electrons and Holes*

a) Show that, for a sample containing N_{n} electrons and N_{p} holes per unit volume with the corresponding mobilities μ_{n} and μ_{p}, the equations for the current density in the presence of applied electric field $\boldsymbol{F}$ and magnetic field B_z are

$$j_x = (\alpha_{\text{n}} + \alpha_{\text{p}})F_x - (\beta_{\text{n}} + \beta_{\text{p}})B_z F_y,$$

$$j_y = (\alpha_{\text{n}} + \alpha_{\text{p}})F_y + (\beta_{\text{n}} + \beta_{\text{p}})B_z F_x,$$

$$j_z = \sigma_0 F_x,$$

where $\alpha_i = N_i e \mu_i$ and $\beta_i = -\alpha_i \mu_i / c$ (delete c for SI units) for i = n and p.

b) Assume that $j_y = 0$, as in a conventional Hall effect measurement, and derive F_y. Calculate the Hall coefficient $R_{\text{H}} = F_y/(j_x B_z)$.

5.7 *Hall Factor in the Limit of Strong and Weak Magnetic Fields*

Show that the Hall coefficient for electrons with a distribution of energies and scattering times τ is given by:

$$R_{\text{H}} = -\frac{\gamma}{\alpha^2}\left[1 + \frac{\gamma^2 B_z^2}{\alpha^2}\right]^{-1}$$

where α and γ are defined in (5.89a,b).

SUMMARY

In this chapter we have discussed the transport of charges in semiconductors under the influence of external fields. We have used the *effective mass approximation* to treat the *free carriers* as having classical charge and renormalized masses. We first considered the case of weak fields in which the field does not distort the carrier distribution but causes the entire distribution to move with a *drift velocity*. The drift velocity is determined by the length of time, known as the *scattering time*, over which the carriers can accelerate in the field before they are scattered. We also defined *mobility* as the constant of proportionality between drift velocity and electric field. We calculated the scattering rates for carriers scattered by *acoustic phonons, optical phonons, and ionized impurities*. Using these scattering rates we deduced the *temperature dependence of the carrier mobilities*. Based on this temperature dependence we introduced *modulation doping* as a way to minimize scattering by ionized impurities at low temperatures. We discussed qualitatively the behavior of carriers under high electric fields. We showed that these *hot carriers* do not obey Ohm's law. Instead, their drift velocities at high fields saturate at a constant value known as the saturation velocity. We showed that the saturation velocity is about 10^7 cm/s in most semiconductors as a result of energy and momentum relaxation of carriers by scattering with optical phonons. In a few n-type semiconductors, such as GaAs, the drift velocity can *overshoot* the saturation velocity and exhibit *negative differential resistance*. This is the result of these semiconductors having secondary conduction band valleys whose energies are of the order of 0.1 eV above the lowest conduction band minimum. The existence of negative differential resistance leads to spontaneous current oscillations at microwave frequencies when thin samples are subjected to high electric fields, a phenomenon known as the *Gunn effect*. Under the combined influence of an electric and magnetic field, the transport of carriers in a semiconductor is described by an antisymmetric second rank *magneto-conductivity tensor*. One important application of this tensor is in explaining the *Hall effect*. The *Hall coefficient* provides the most direct way to determine the sign and concentration of charged carriers in a sample.